

## VIBRATIONAL DYNAMICS OF Cu-BASED BINARY GLASSY ALLOYS

Aditya M. Vora

Humanities and Social Science Department, S. T. B. S. College of Diploma Engineering,  
Opp. Spinning Mill, Varachha Road, Surat 395 006, Gujarat, India

Received 16 February, 2010

**Abstract:** The well-recognized model potential is used to investigate the vibrational properties for five Cu-based binary glassy alloys viz.  $\text{Cu}_{57}\text{Zr}_{43}$ ,  $\text{Cu}_{60}\text{W}_{40}$ ,  $\text{Cu}_{33}\text{Y}_{67}$ ,  $\text{Cu}_{43}\text{Ti}_{57}$  and  $\text{Cu}_{66}\text{Ti}_{34}$ . The thermodynamic and elastic properties are also computed from the elastic limits of the PDC. Three theoretical approaches given by Hubbard-Beeby (HB), Takeno-Goda (TG) and Bhatia-Singh (BS) are used in the present study to compute the phonon dispersion curves (PDC). Five local field correction functions proposed by Hartree (H), Taylor (T), Ichimaru-Utsumi (IU), Farid *et al.* (F) and Sarkar *et al.* (S) are employed to see the effect of exchange and correlation in the aforesaid properties.

**Keywords:** pseudopotential; pair potential; phonon dispersion curves; Cu-based binary glassy alloys

### 1. Introduction

The research on intertransition metals-based binary alloys has followed from the desire to understand the mechanisms responsible for their physical and electronic properties. Examples of significant problems include the conditions under which amorphous or crystalline phases form, and the technological origins of negative temperature coefficients of electrical resistance. At a basic level all of these properties must be controlled by the electronic structure of the valence electrons. Theoretical understanding of these structures has been difficult to achieve because of the lack of translational symmetry, both for disordered crystalline alloys and amorphous or glassy alloys. The possible application of transition metal alloys is in microelectronics or as thin-film coating [1-9].

All the Cu-glassy alloys are the member of the transition metal- transition metal (TM-TM) element group. The PDC of  $\text{Cu}_{57}\text{Zr}_{43}$  glass was also studied by Agarwal *et al.* [10] using Bhatia-Singh (BS) [11] approach and various types of screening. While the PDC of  $\text{Cu}_{66}\text{Ti}_{34}$  glass was reported by Gupta *et al.* [12]. The photoemission and electronic structural analysis of  $\text{Cu}_{60}\text{W}_{40}$  glass have been studied by Engelhardt *et al.* [13]. The vibrational dynamics of  $\text{Cu}_{60}\text{W}_{40}$ ,  $\text{Cu}_{33}\text{Y}_{67}$  and  $\text{Cu}_{43}\text{Ti}_{57}$  metallic glasses is not reported previously using model potential formalism. Recently, Vora *et al.* [1-9] have reported the vibrational properties of some metallic glasses using model potential formalism.

Looking to the advantages of metallic glasses, the present paper is emphasized the vibrational dynamics of five Cu-based binary glassy alloys viz.  $\text{Cu}_{57}\text{Zr}_{43}$ ,  $\text{Cu}_{60}\text{W}_{40}$ ,  $\text{Cu}_{33}\text{Y}_{67}$ ,  $\text{Cu}_{43}\text{Ti}_{57}$  and  $\text{Cu}_{66}\text{Ti}_{34}$  using well-recognized model potential [1-9] for the first time. The thermodynamics and elastic properties of such as longitudinal sound velocity  $v_L$ , transverse sound velocity  $v_T$ , isothermal bulk modulus  $B_T$ , modulus of rigidity  $G$ , Poisson's ratio  $\sigma$ , Young's modulus  $Y$  and Debye temperature  $\theta_D$  are computed from the elastic limit of the dispersion relation. Five different

types of local field correction functions proposed by Hartree (H) [14], Taylor (T) [15], Ichimaru-Utsumi (IU) [16], Farid et al. (F) [17] and Sarkar et al. (S) [18] are used to study the exchange and correlation effects in the aforesaid studies. The phenomenological theories of Hubbard-Beeby (HB) [19], Takeno-Goda (TG) [20] and Bhatia-Singh (BS) [11, 21] are employed to generate the phonon dispersion curves (PDC). The most important ingredient of the PDC is pair potential computed theoretically in Wills-Harrison (WH) [22] form from well-recognized model potential [1-9].

## 2. Theoretical Methodology

The fundamental ingredient, which goes into the calculation of the phonon dynamics of metallic glasses, is the pair potential. In the present study, for TM-TM, the pair potential is computed using [1-9, 22]

$$V(r) = V_s(r) + V_b(r) + V_r(r). \quad (1)$$

The *s*-electron contribution to the pair potential  $V_s(r)$  is calculated from

$$V_s(r) = (Z_s^2 e^2 / r) + (\Omega_o / \pi^2) \int F(q) [\sin(qr) / qr] q^2 dq. \quad (2)$$

Here  $Z_s \sim 1.5$  is found by integrating the partial *s*-density of states resulting from self-consistent band structure calculation for the entire 3d and 4d series [22], while  $\Omega_o$  the effective atomic volume of the one component fluid.

The energy wave number characteristics appearing in Eq. (2) is written as [1-9, 22]

$$F(q) = (-\Omega_o q^2 / 16\pi) |W_B(q)|^2 [\varepsilon_H(q) - 1] / \{1 + [\varepsilon_H(q) - 1][1 - f(q)]\}. \quad (3)$$

Here  $W_B(q)$  is the effective bare ion potential,  $\varepsilon_H(q)$  the Hartree dielectric response function and  $f(q)$  the local field correction function to introduce the exchange and correlation effects.

The well-recognized model potential  $W_B(q)$  [1-9] used in the present computation of phonon dynamics of binary metallic glasses is of the form

$$W_B(q) = \frac{-4\pi e^2 Z}{\Omega_o q^2} \left[ \begin{array}{l} \left\{ -1 + \frac{12}{U^2} + \frac{U^2}{1+U^2} + \frac{6U^2}{(1+U^2)^2} + \frac{18U^2}{(1+U^2)^3} - \frac{6U^4}{(1+U^2)^3} \right\} \cos(U) \\ + \left\{ \frac{24U^2}{(1+U^2)^4} - \frac{24U^4}{(1+U^2)^4} \right\} \\ + \\ \left\{ \frac{6}{U} - \frac{12}{U^3} + \frac{U}{1+U^2} + \frac{3U}{(1+U^2)^2} - \frac{3U^3}{(1+U^2)^2} + \frac{6U}{(1+U^2)^3} \right\} \sin(U) \\ - \left\{ \frac{18U^3}{(1+U^2)^3} + \frac{6U}{(1+U^2)^4} - \frac{36U^3}{(1+U^2)^4} + \frac{6U^5}{(1+U^2)^4} \right\} \\ + \\ 24U^2 \exp(1) \left\{ \frac{U^2 - 1}{(1+U^2)^4} \right\} \end{array} \right]. \quad (4)$$

Here  $U = qr_c$ .  $r_c$  is the model potential parameter. This form has feature of a Coulombic term outside the core and varying cancellation due to repulsive and attractive contributions to the potential within the core in real space. The detailed information of this potential is given in the literature [1-9]. The model potential parameter  $r_c$  is calculated from the well-known formula [1-9] as follows :

$$r_c = \left[ \frac{0.51 r_s}{(Z)^{1/3}} \right]. \quad (5)$$

Here  $r_s$  is the Wigner-Seitz radius of the amorphous alloys.

The  $d$ -electron contributions to the pair potential are expressed in terms of the number of  $d$ -electron  $Z_d$ , the  $d$ -state radii  $r_d$  and the nearest-neighbor coordination number  $N_c$  as follows:

$$V_b(r) = -Z_d \left( 1 - \frac{Z_d}{10} \right) \left( \frac{12}{N_c} \right)^{1/2} \left( \frac{28.06}{\pi} \right) \frac{2r_d^3}{r^5}, \quad (6)$$

and

$$V_r(r) = Z_d \left( \frac{450}{\pi^2} \right) \frac{r_d^6}{r^8}. \quad (7)$$

The theories of Hubbard-Beeby (HB) [19], Takeno-Goda (TG) [20] and Bhatia-Singh (BS) [11, 21] have been employed in the present computation. The expressions for longitudinal phonon frequency  $\omega_L$  and transverse phonon frequency  $\omega_T$  as per HB, TG and BS approaches are given below [11, 19-21].

According to the Hubbard-Beeby (HB) [19], the expressions for longitudinal phonon frequency  $\omega_L$  and transverse phonon frequency  $\omega_T$  are

$$\omega_L^2(q) = \omega_E^2 \left[ 1 - \frac{\sin(q\sigma)}{q\sigma} - \frac{6 \cos(q\sigma)}{(q\sigma)^2} + \frac{6 \sin(q\sigma)}{(q\sigma)^3} \right], \quad (8)$$

and

$$\omega_T^2(q) = \omega_E^2 \left[ 1 - \frac{3 \cos(q\sigma)}{(q\sigma)^2} + \frac{3 \sin(q\sigma)}{(q\sigma)^3} \right] \quad (9)$$

with  $\omega_E^2 = \left( \frac{4\pi\rho}{3M} \right) \int_0^\infty g(r)V''(r)r^2 dr$  being the maximum frequency.

The theory for computing the phonon dynamics in amorphous solids, approach proposed by Takeno-Goda (TG) [20] has been employed in the present computation. The expressions for longitudinal phonon frequency  $\omega_L$  and transverse phonon frequency  $\omega_T$  are

$$\omega_L^2(q) = \left(\frac{4\pi\rho}{M}\right) \int_0^\infty dr g(r) \left[ \left\{ rV'(r) \left(1 - \frac{\sin(qr)}{qr}\right) \right\} + \left\{ r^2V''(r) - rV'(r) \right\} \left( \frac{1}{3} - \frac{\sin(qr)}{qr} - \frac{2\cos(qr)}{(qr)^2} + \frac{2\sin(qr)}{(qr)^3} \right) \right], \quad (10)$$

and

$$\omega_T^2(q) = \left(\frac{4\pi\rho}{M}\right) \int_0^\infty dr g(r) \left[ \left\{ rV'(r) \left(1 - \frac{\sin(qr)}{qr}\right) \right\} + \left\{ r^2V''(r) - rV'(r) \right\} \left( \frac{1}{3} + \frac{2\cos(qr)}{(qr)^2} + \frac{2\sin(qr)}{(qr)^3} \right) \right]. \quad (11)$$

Here  $M$ ,  $\rho$  are the atomic mass and the number density of the glassy alloy while  $V''(r)$  is the second derivative of the pair potential, respectively.

Recently Bhatia-Singh (BS) [11] was modified by Shukla and Campnaha [21]. They were introduced screening effects in the BS approach. Then, with the above assumptions and modification, the dispersion equations for an amorphous material can be written as [11, 21]

$$\rho\omega_L^2(q) = \frac{2N_C}{q^2} (\beta I_0 + \delta I_2) + \frac{k_e k_{TF}^2 q^2 \varepsilon(q) |G(qr_s)|^2}{q^2 + k_{TF}^2 \varepsilon(q)}, \quad (12)$$

and

$$\rho\omega_T^2(q) = \frac{2N_C}{q^2} \left( \beta I_0 + \frac{1}{2} \delta (I_0 - I_2) \right). \quad (13)$$

Other details of used constants in the BS approach were already narrated in the literature [11, 21]. Here  $M$  is the effective atomic mass,  $\rho$  the effective number density and  $N_C$  the effective coordination number of the glassy system, respectively.

In the long-wavelength limit of the frequency spectrum, both phonon frequencies viz. the longitudinal  $\omega_L$  and transverse  $\omega_T$  phonon frequencies are proportional to the wave vectors and obey the relationships [1-9, 11, 19-21],

$$\omega_L \propto q \text{ and } \omega_T \propto q, \therefore \omega_L = v_L q \text{ and } \omega_T = v_T q, \quad (14)$$

where,  $v_L$  and  $v_T$  are the longitudinal and transverse sound velocities of the glassy alloys, respectively. Detail expressions of the long-wavelength limit of the frequency spectrum are narrated in our earlier papers [1-9].

The present study also includes isothermal bulk modulus  $B_T$ , modulus of rigidity  $G$ , Poisson's ratio  $\sigma$ , Young's modulus  $Y$  and Debye temperature  $\theta_D$  from the elastic limit of the

PDC. All the quantities are computed from the longitudinal and transverse sound velocities ( $v_L$  and  $v_T$ ). The bulk modulus  $B_T$ , modulus of rigidity  $G$ , Poisson's ratio  $\sigma$ , Young's modulus  $Y$  and Debye temperature  $\theta_D$  are obtained using the expressions [1-9]:

$$B_T = \rho_M \left( v_L^2 - \frac{4}{3} v_T^2 \right), \quad (15)$$

$$G = \rho_M v_T^2, \quad (16)$$

with  $\rho_M$  is the isotropic number density of the solid.

$$\sigma = \frac{1 - 2(v_T^2/v_L^2)}{2 - 2(v_T^2/v_L^2)}, \quad (17)$$

$$Y = 2G(\sigma + 1), \quad (18)$$

and

$$\theta_D = \frac{\hbar \omega_D}{k_B} = \frac{\hbar}{k_B} 2\pi \left[ \frac{9\rho}{4\pi} \right]^{1/3} \left[ \frac{1}{v_L^3} + \frac{2}{v_T^3} \right]^{(-1/3)}. \quad (19)$$

The low temperature specific heat  $C_V$  can be calculated from the following expression [23]:

$$C_V = \frac{\Omega_o \hbar^2}{k_B T^2} \sum_{\lambda=L,T} \frac{d^3 q}{(2\pi)^3} \frac{\omega_\lambda^2(q)}{\left[ \exp\left(\frac{\hbar \omega_\lambda(q)}{k_B T}\right) - 1 \right] \left[ 1 - \exp\left(\frac{\hbar \omega_\lambda(q)}{k_B T}\right) \right]}. \quad (20)$$

Here  $\hbar$ ,  $k_B$ ,  $\omega_D$  are the Plank's constant, Boltzmann's constant and Debye frequency, respectively.

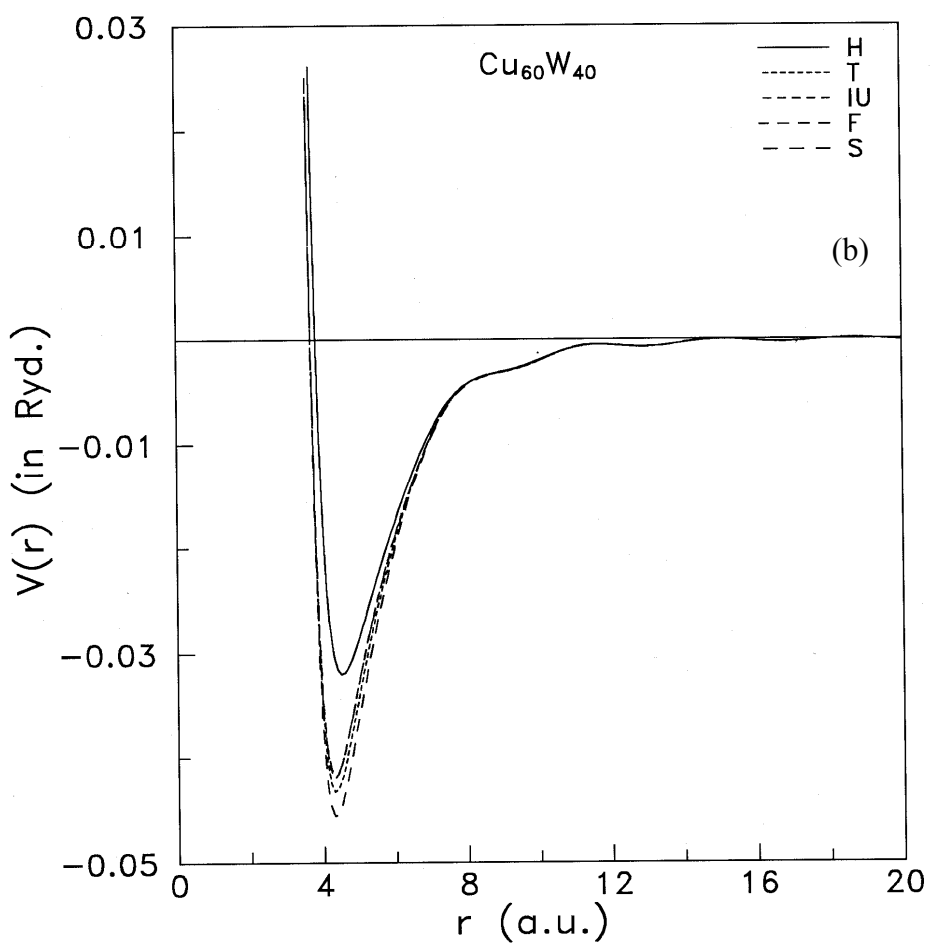
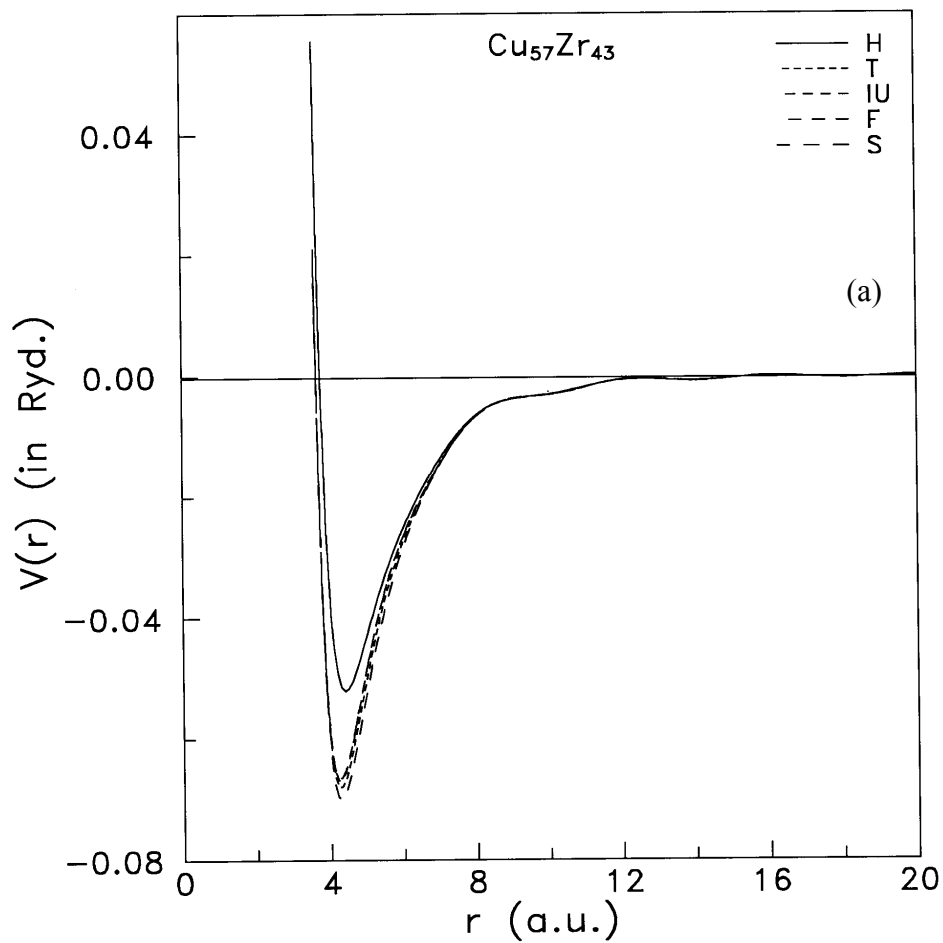
### 3. Results and Discussion

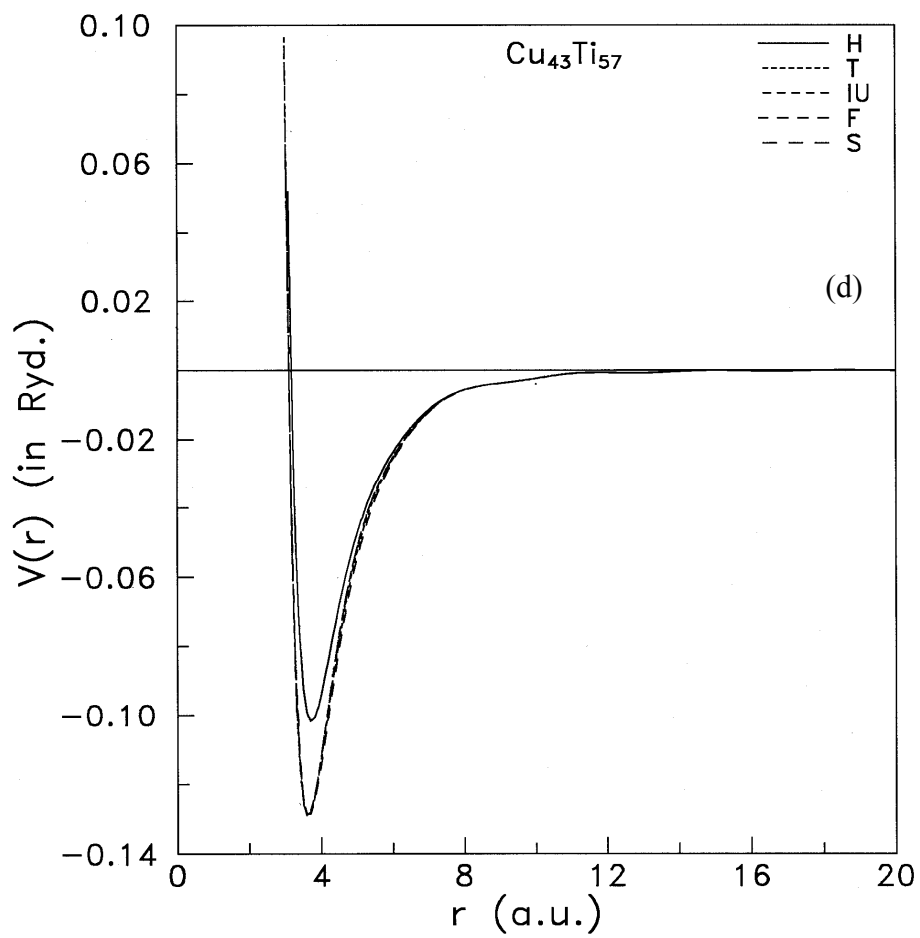
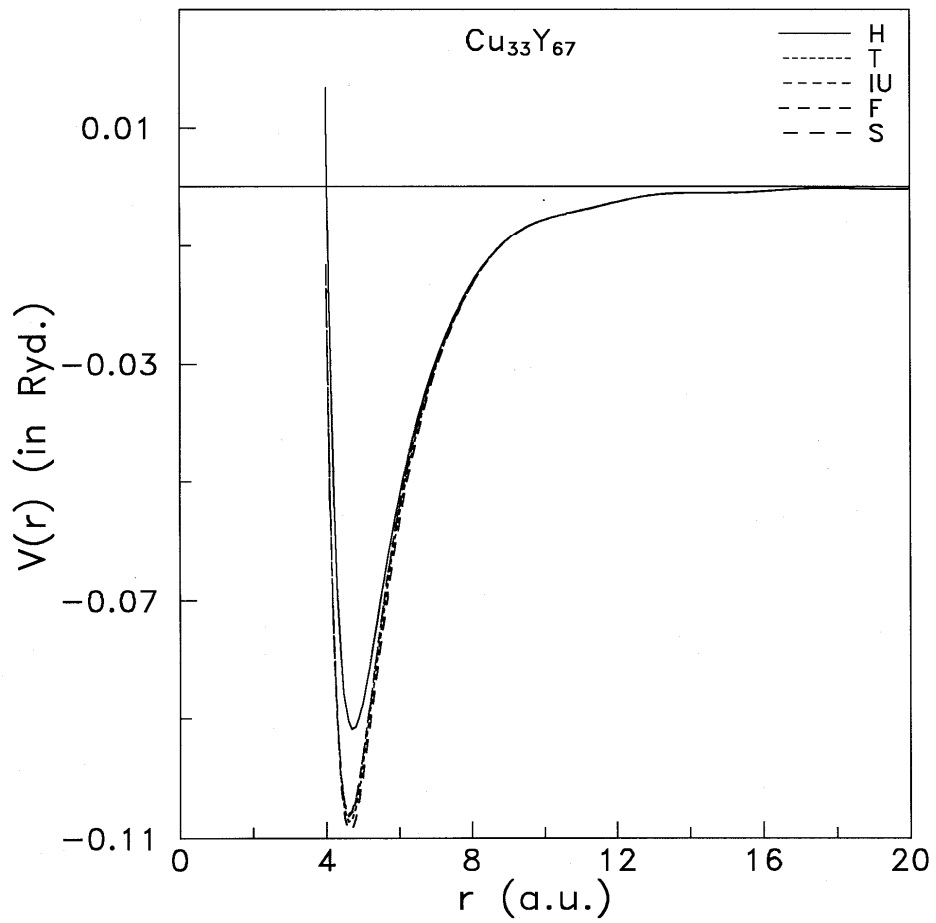
The input parameters and other related constants used in the present computations are tabulated in table 1 (they are taken from the literature [22]).

**Table 1.** Input parameters and other constants.

Glasses	Z	$\Omega_o$ (au)	$r_c$ (au)	$Z_d$	$N_c$	$r_d$ (au)
<b>Cu<sub>57</sub>Zr<sub>43</sub></b>	3.01	158.44	0.8673	6.49	12.00	1.87
<b>Cu<sub>60</sub>W<sub>40</sub></b>	3.00	160.48	0.8327	7.50	10.40	1.72
<b>Cu<sub>33</sub>Y<sub>67</sub></b>	2.34	126.09	1.0090	4.14	12.00	2.42
<b>Cu<sub>43</sub>Ti<sub>57</sub></b>	2.71	114.47	0.8409	5.51	12.00	1.71
<b>Cu<sub>66</sub>Ti<sub>34</sub></b>	2.02	90.61	0.9923	7.12	12.00	1.53

The computed data of pair potentials of  $\text{Cu}_{57}\text{Zr}_{43}$  glass are shown in Figure 1(a). The position of pair potential at  $r = r_0$  due to H-screening occurs at  $r_0 = 3.7$  au, while the inclusion of exchange and correlation suppresses the first zero  $V(r = r_0)$  of the pair potential at  $r_0 \leq 3.6$  au. The presently calculated pair potentials  $\text{Cu}_{60}\text{W}_{40}$  glassy alloy of are shown in Figure 1(b). It is seen that the exchange and correlation effects affect largely the behavior of the pair potential. The first zero of pair potential at  $r = r_0$  due to H-screening occurs at  $r_0 = 3.8$  au, while inclusion of exchange and correlation suppresses this zero to  $r_0 \leq 3.6$  au. The present results show very small oscillations in the large  $r$ -region. The presently computed pair potentials of  $\text{Cu}_{33}\text{Y}_{67}$  glass are drawn in Figure 1(c). It is seen that the exchange and correlation functions affect the nature of the pair potential as well as the first zero of  $V(r)$  appreciably. The position of  $V(r = r_0)$  due to H-screening occurs at  $r_0 = 4.0$  au, while the effect of screening suppresses this zero to  $r_0 \leq 3.8$  au. The computed pair potentials of  $\text{Cu}_{43}\text{Ti}_{57}$  glass are displayed in Figure 1(d). It is observed that the nature of the pair potentials change appreciably with inclusion of exchange and correlation effects. The first zero for  $V(r = r_0)$  due to all the screenings occurs at  $r_0 \approx 3.1$  au. The present results do not show any oscillations in the large  $r$ -region. The WH form of pair potentials of  $\text{Cu}_{66}\text{Ti}_{34}$  glass has been computed to see the atomic interactions and displayed in Figure 1(e). It is apparent that the position of the first minimum, well width and well depth of the pair potential is highly affected by various screening functions. The first zero of  $V(r = r_0)$  due to H-screening occurs at  $r_0 = 3.5$  au, while inclusion of exchange and correlation suppresses this zero to  $r_0 \leq 3.2$  au. It is seen that well depth of presently computed potentials moves towards the left in contrast to the pair potential of Gupta *et al.* [12]. Also the pair potentials do not show any significant oscillations and almost constant in the large  $r$ -region. The presently calculated pair potentials of all glassy alloys elucidate that the inclusion of screening functions hardly changes the nature of the pair potentials, except around the first minimum. The well depth slightly increases due to influence of various screening functions compared to H-screening. The maximum depth in the pair potential is obtained for S-function. The pair potentials due to remaining T, IU and F-screening functions are lying between those of H and S-screening functions. Also, the present results of pair potentials of all Cu-based glassy alloys do not show any oscillatory behavior and almost constant in the large  $r$ -region. The presently computed pair potentials from H, T IU, F and S-local field correction functions for most of the amorphous alloys are overlapped with each other.





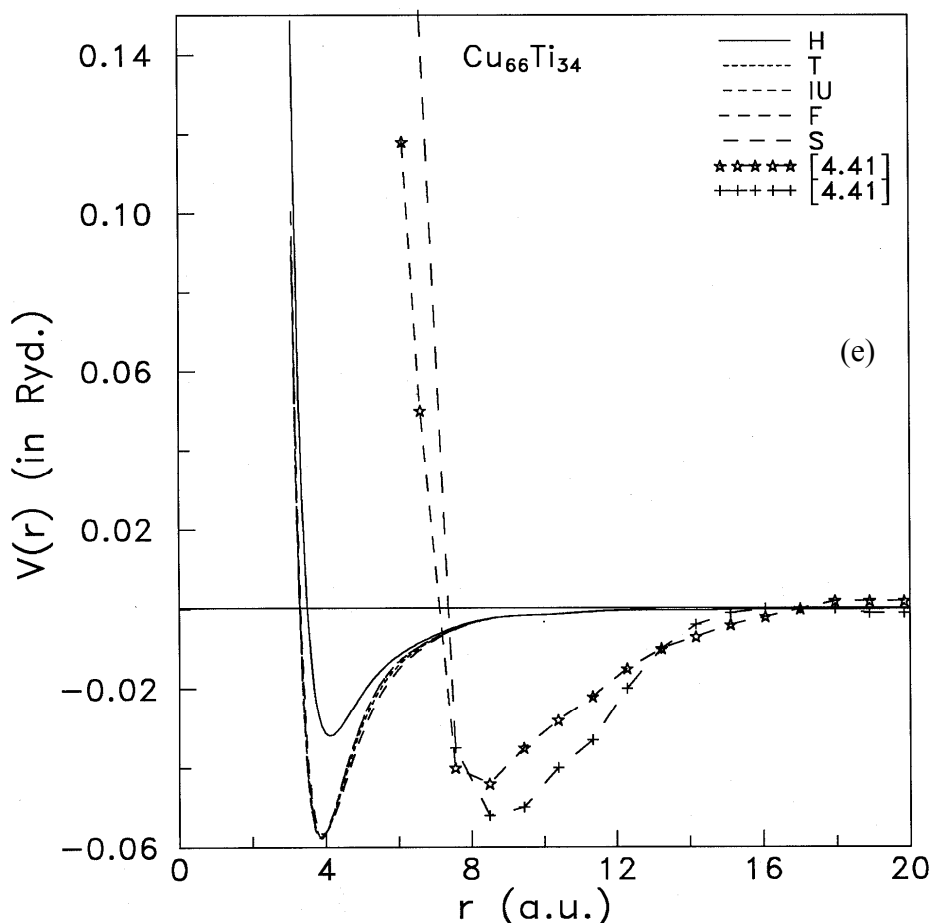
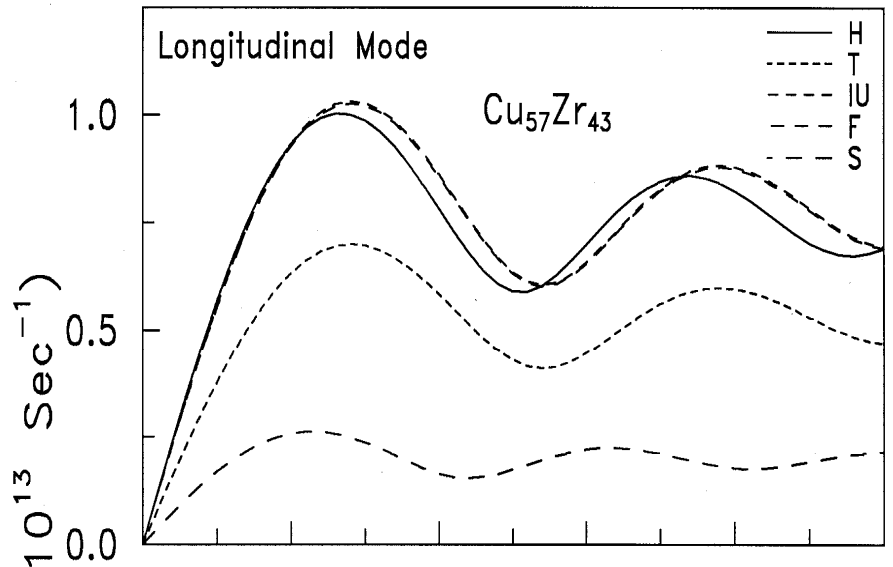


Fig. 1. Pair potentials for (a)  $\text{Cu}_{57}\text{Zr}_{43}$ , (b)  $\text{Cu}_{60}\text{W}_{40}$ , (c)  $\text{Cu}_{33}\text{Y}_{67}$ , (d)  $\text{Cu}_{43}\text{Ti}_{57}$  and (e)  $\text{Cu}_{66}\text{Ti}_{34}$  metallic glasses.

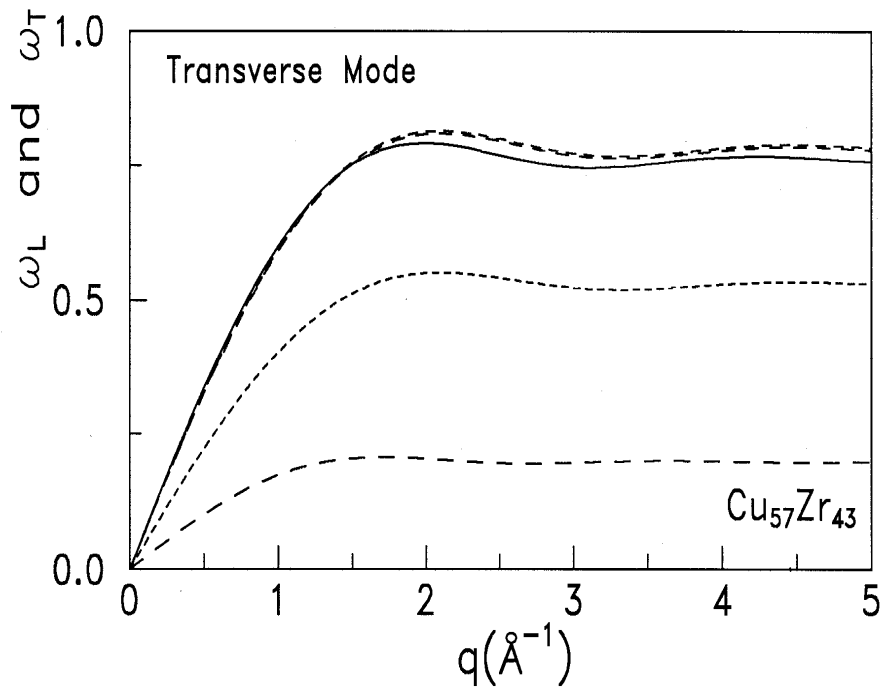
From the Figures 1(a)–(e), it is observed that the shifting of the pair potentials with respect to atomic volume  $\Omega_o$  of the amorphous alloys. The repulsive Coulomb interaction and the attractive interactions represented by oscillatory nature are observed. It is also noticed that when volume  $\Omega_o$  of the glassy alloys increases ( $\Omega_o$  is more for  $\text{Cu}_{60}\text{W}_{40}$  glass), the potential depth deepens. It means that the pair potential for  $\text{Cu}_{60}\text{W}_{40}$  glass shows higher depth in comparison with other metallic glasses. All the pair potentials show the combined effect of the s- and d-electrons. Bretonnet and Derouiche [24] are observed that the repulsive part of  $V(r)$  is drawn lower and its attractive part is deeper due to the d-electron effect. When we go from  $\text{Cu}_{43}\text{Ti}_{57} \rightarrow \text{Cu}_{33}\text{Y}_{67}$ , the net number of d-electron  $r_d$  decreases, hence the  $V(r)$  is shifted towards the lower  $r$ -values. Therefore, the present results support the d-electron effect as noted by Bretonnet and Derouiche [19]. Also, from Figures 1(a)–(e), it can be noted that the Coulomb repulsive potential part dominates the oscillations due to ion-electron-ion interactions, which shows the waving shape oscillation of the potential after  $r \approx 10$  au. Hence, the pair potentials are converged towards a finite value instead of zero in the repulsive region.

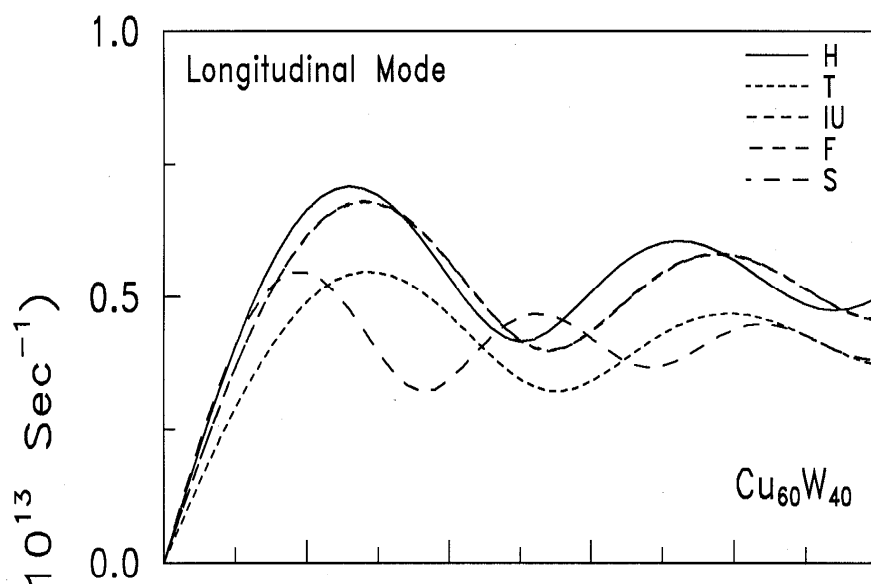
The phonon modes for longitudinal and transverse branches of  $\text{Cu}_{57}\text{Zr}_{43}$ ,  $\text{Cu}_{60}\text{W}_{40}$ ,  $\text{Cu}_{33}\text{Y}_{67}$ ,  $\text{Cu}_{43}\text{Ti}_{57}$  and  $\text{Cu}_{66}\text{Ti}_{34}$  metallic glasses calculated using HB approach with the five screening functions are shown in figures 2(a)-(e). To study the screening influence on the phonon eigen frequencies, the longitudinal and transverse phonon modes obtained using HB approach are shown in Figure 2(a) for  $\text{Cu}_{57}\text{Zr}_{43}$  glass. The enhancement in both the phonon branches is concluded due to the effect of exchange and correlation functions. The present results of PDC due to H, T and F are lying between those due to IU and S-screening. The first minimum in the longitudinal branch for H, T, IU, F and S-local field correction functions occurs at  $q \approx 2.6 \text{ \AA}^{-1}$ ,  $2.7 \text{ \AA}^{-1}$ ,  $2.7 \text{ \AA}^{-1}$ ,  $2.7 \text{ \AA}^{-1}$  and  $1.7 \text{ \AA}^{-1}$ , respectively. At first peak, the screening influence on  $\omega_L$  with respect to H-screening is 30.26% in the case of T-function, 2.89% in the case of IU-function, 2.33% in the case of F-function and 28.32% in the case of S-function. Such influence on  $\omega_T$  at  $q \approx 1.0 \text{ \AA}^{-1}$  point due to T-screening is 33.06%, for IU is 1.23%, for F is 1.76% and for S-screening is 71.20% with respect to H-dielectric function. Figure 2(b) shows the phonon frequencies for  $\text{Cu}_{60}\text{W}_{40}$  glass obtained for various local field correction functions. It is seen that the first minimum in the longitudinal branch for H, T, IU, F and S-local field correction functions occurs at  $q \approx 2.5 \text{ \AA}^{-1}$ ,  $2.8 \text{ \AA}^{-1}$ ,  $2.7 \text{ \AA}^{-1}$ ,  $2.7 \text{ \AA}^{-1}$  and  $1.8 \text{ \AA}^{-1}$ , respectively. At first maximum, the screening influence on  $\omega_L$  is 3.92% to 22.97% with respect to static function of Hartree (H). Such influence on  $\omega_T$  at  $q \approx 1.0 \text{ \AA}^{-1}$  point is 7.21% to 27.70%. The longitudinal and transverse phonon frequencies of  $\text{Cu}_{33}\text{Y}_{67}$  glass calculated using HB approach to study the screening influence is shown in Figure 2(c). It is seen that the influence of exchange and correlation effect lowers the phonon frequencies except for S-local field correction function. The first minimum in the longitudinal branch for H, T, IU, F and S-screening occurs at  $q \approx 2.3 \text{ \AA}^{-1}$ ,  $2.5 \text{ \AA}^{-1}$ ,  $2.4 \text{ \AA}^{-1}$ ,  $2.4 \text{ \AA}^{-1}$  and  $2.9 \text{ \AA}^{-1}$ , respectively. The suppression of  $\omega_L$  at first peak due to T-dielectric function is 80.43%, for IU is 15.16% and for F is 17.83% with respect to H-dielectric function. The S-screening rises  $\omega_L$  at first peak by 22.92% with respect to H-dielectric function. At  $q \approx 1.0 \text{ \AA}^{-1}$  position, the screening influence on  $\omega_T$  due to T, IU, F and S-screening is 27.70%, 9.14%, 8.86% and 7.2%, respectively with respect to H-dielectric function. The screening influence on phonon frequencies of  $\text{Cu}_{43}\text{Ti}_{57}$  glass is shown in Figure 2(d) where the results due to HB approach are included. It is apparent that both the longitudinal and transverse phonon frequencies lower by the inclusion of exchange and correlation effects. The first minimum in the longitudinal branch for H, T, IU, F and S-local field correction functions lies at  $q \approx 2.9 \text{ \AA}^{-1}$ ,  $3.1 \text{ \AA}^{-1}$ ,  $3.0 \text{ \AA}^{-1}$ ,  $3.0 \text{ \AA}^{-1}$  and  $3.1 \text{ \AA}^{-1}$ , respectively. The screening influence on longitudinal frequencies at first maximum is 24.40% for T, 7.98% for IU, 8.83% for F and 33.45% for S-screening with respect to H-screening. While such influence at  $q \approx 1.0 \text{ \AA}^{-1}$  point on  $\omega_T$  due to T, IU, F and S-screening is

26.90%, 9.43%, 10.25% and 18.45%, respectively. In the present study the phonon frequencies of  $\text{Cu}_{66}\text{Ti}_{34}$  glass, calculated using HB approach with the five screening functions are shown in Figure 2(e). It is noticed that both the phonon modes are very sensitive to the screening effect. The first depth in the longitudinal branch for H, T, IU, F and S-local field correction functions is around  $q \approx 2.7 \text{ \AA}^{-1}$ ,  $2.8 \text{ \AA}^{-1}$ ,  $2.8 \text{ \AA}^{-1}$ ,  $2.8 \text{ \AA}^{-1}$  and  $3.0 \text{ \AA}^{-1}$ , respectively. The screening influence on  $\omega_L$  with respect to H-screening is 5.38% for T, 20.49% for IU, 19.67% for F and 8.92% for S-screening. At  $q \approx 1.0 \text{ \AA}^{-1}$  point, the influence on  $\omega_T$  due to T, IU, F and S-screening is 9.32%, 17.18%, 16.38% and 16.75%, respectively.

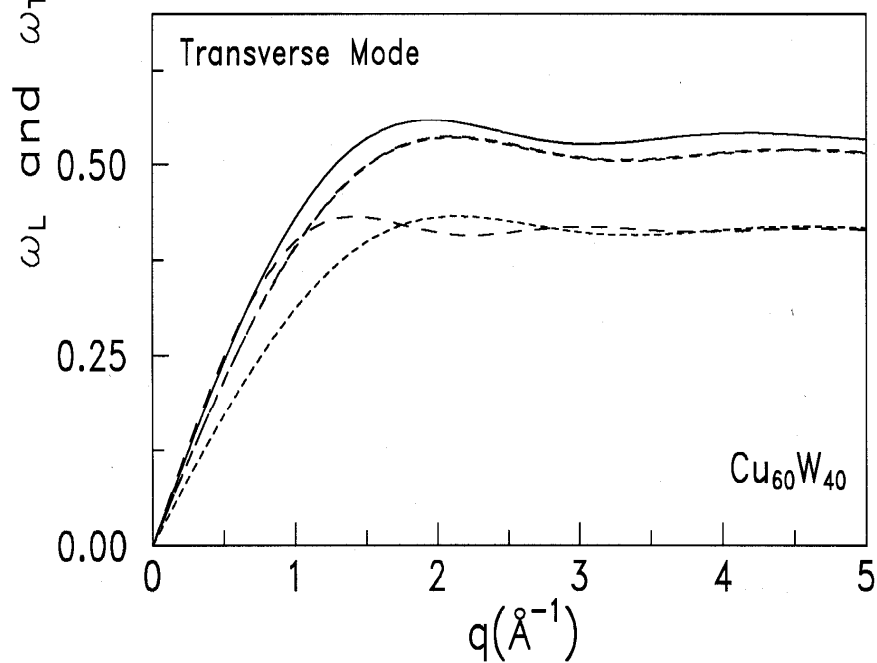


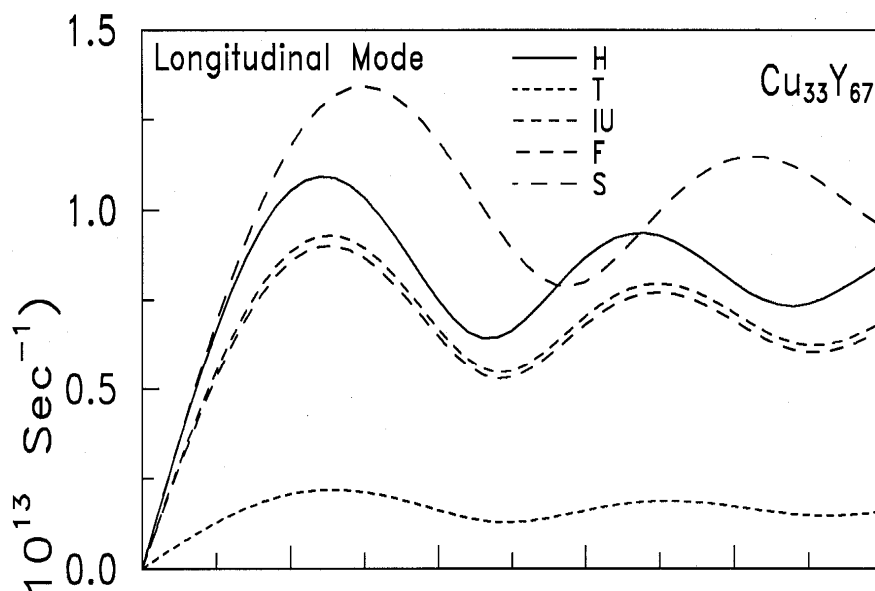
(a)



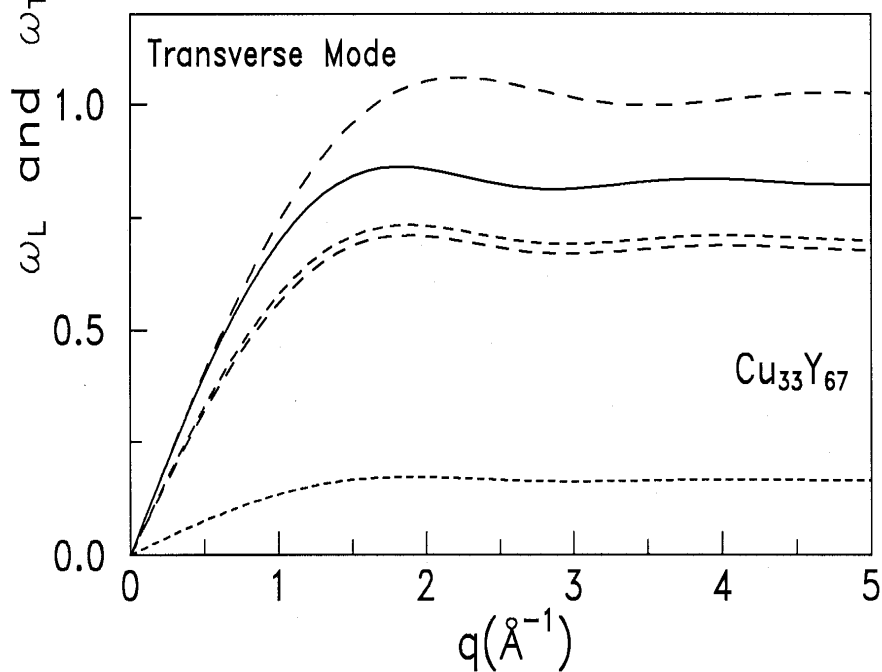


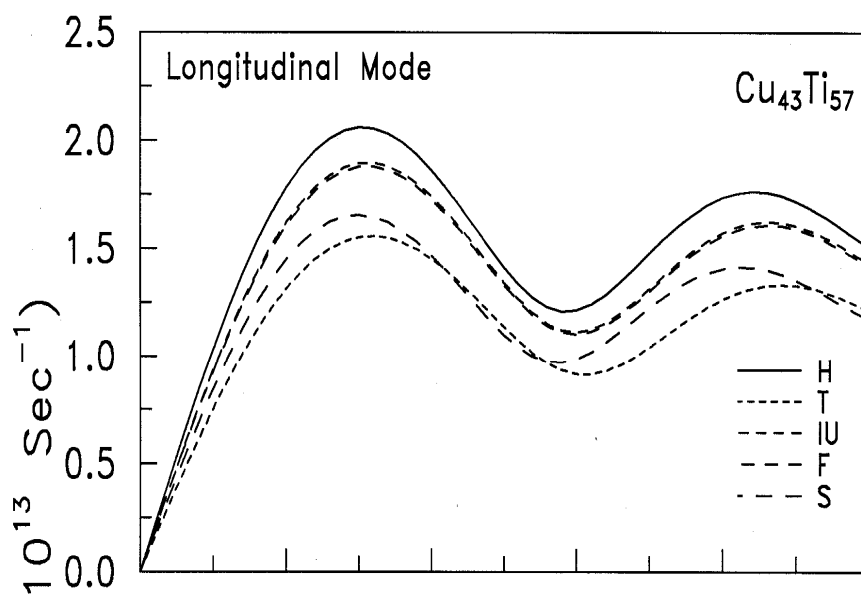
(b)



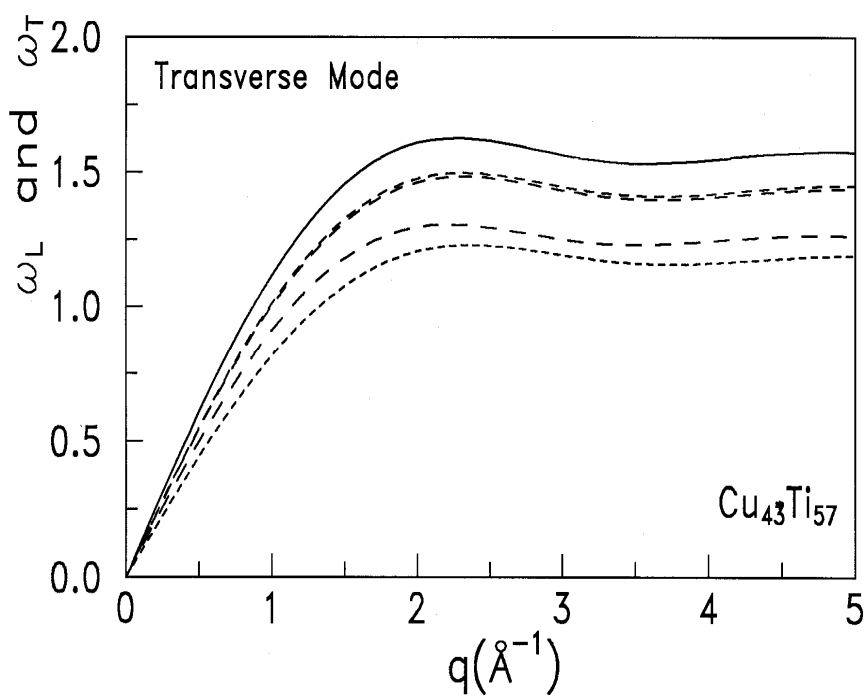


(c)





(d)



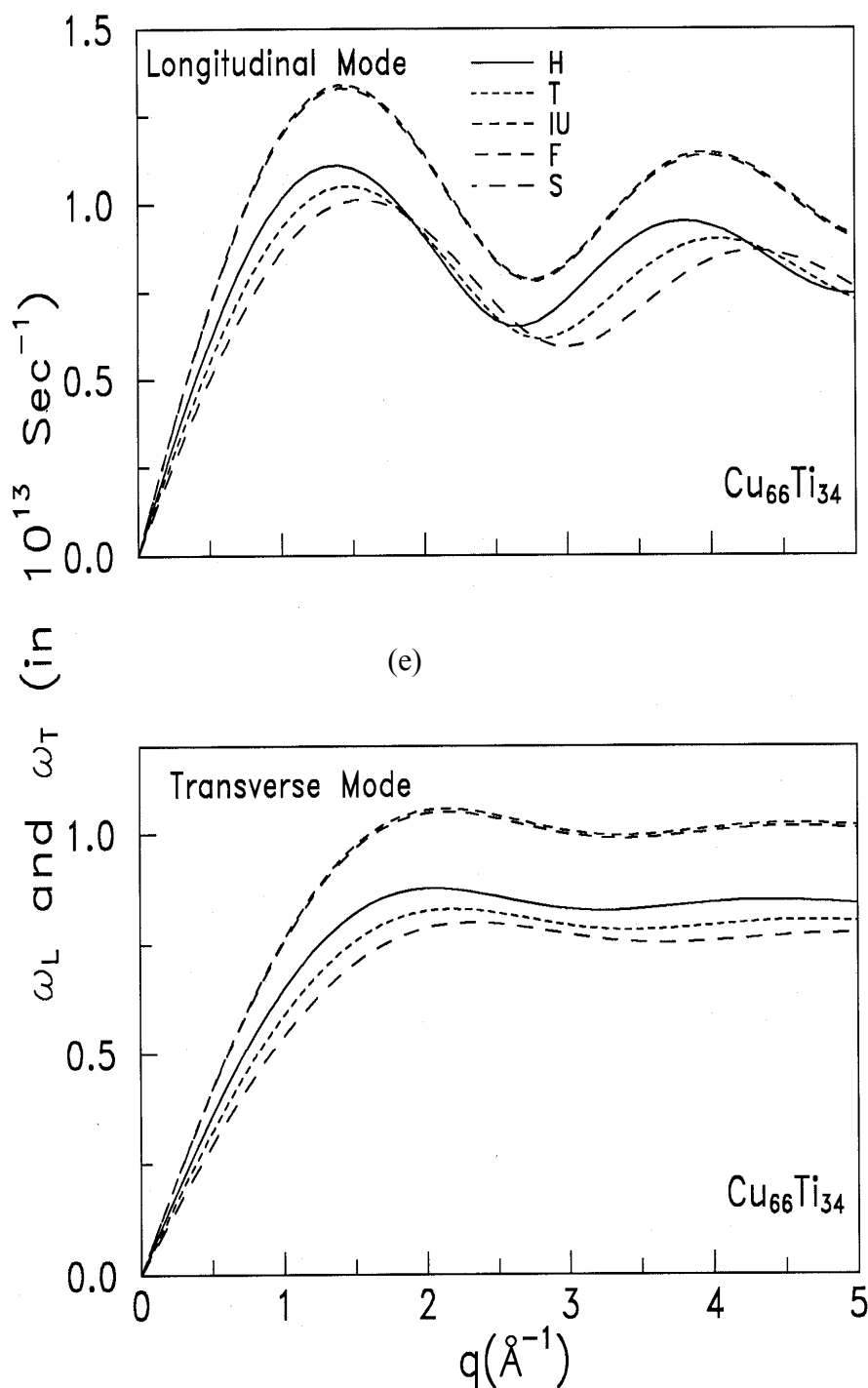


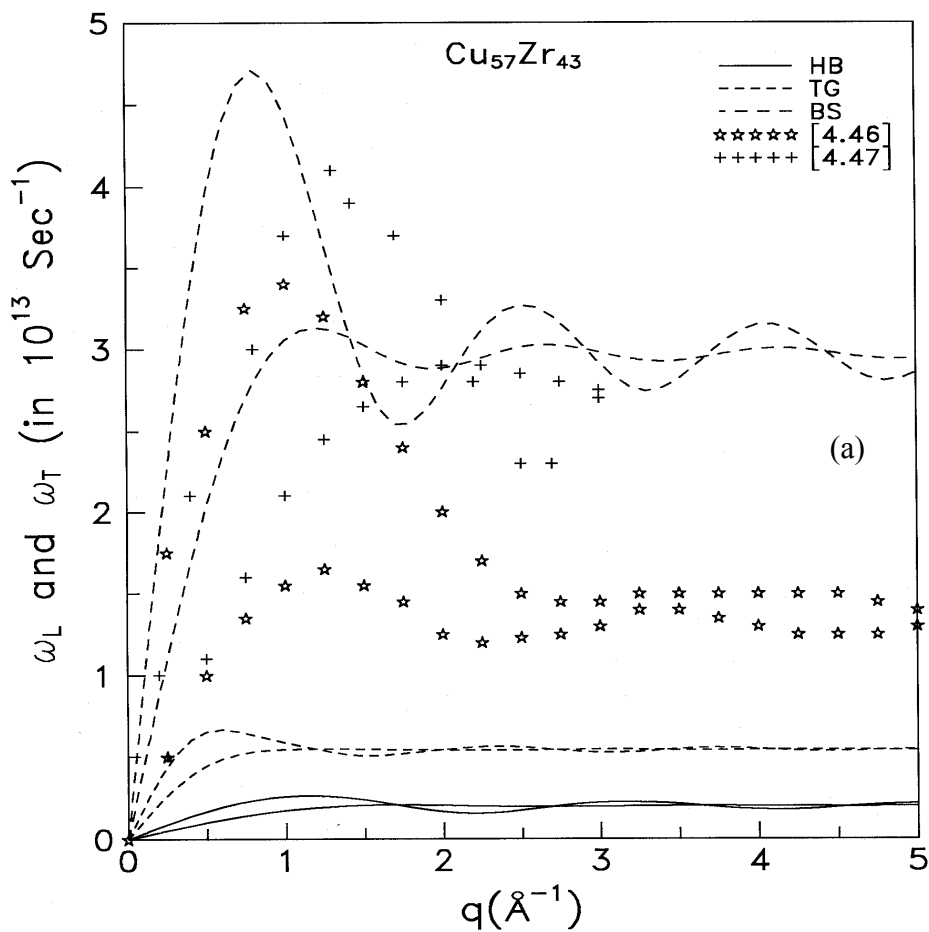
**Fig. 2.** Screening dependence of the phonon dispersion curves for (a)  $\text{Cu}_{57}\text{Zr}_{43}$ , (b)  $\text{Cu}_{60}\text{W}_{40}$ , (c)  $\text{Cu}_{33}\text{Y}_{67}$ , (d)  $\text{Cu}_{43}\text{Ti}_{57}$  and (e)  $\text{Cu}_{66}\text{Ti}_{34}$  metallic glasses using HB approach.

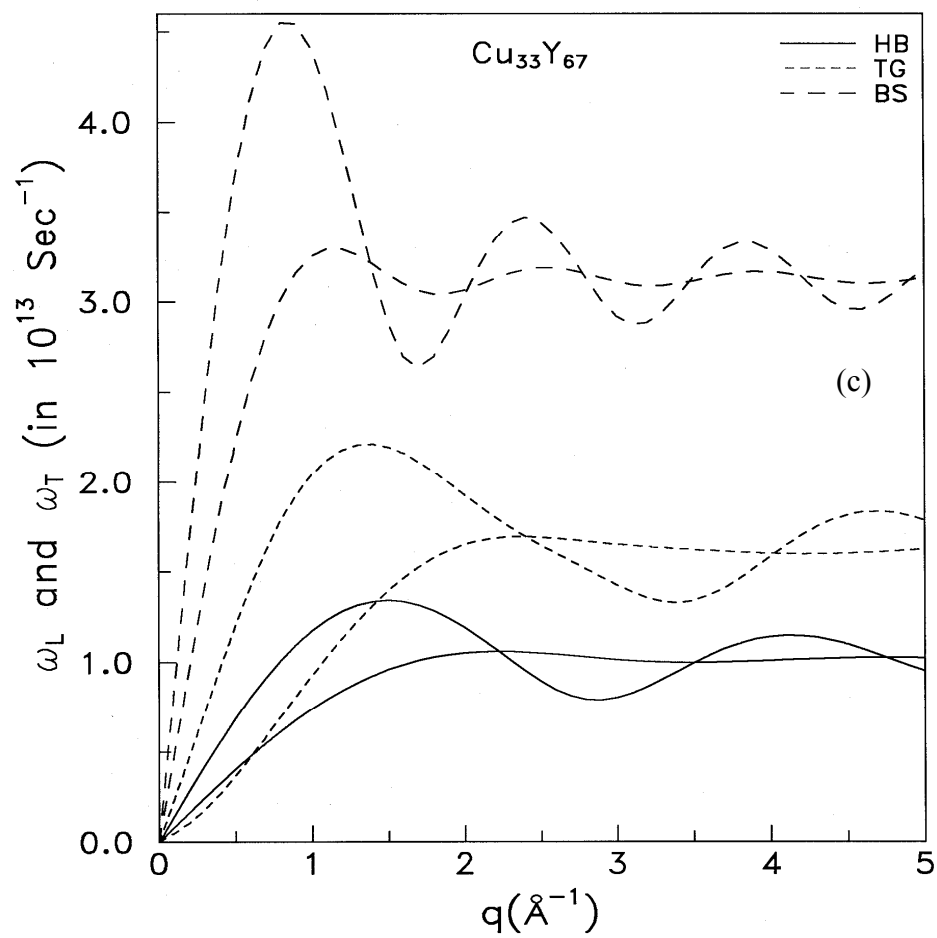
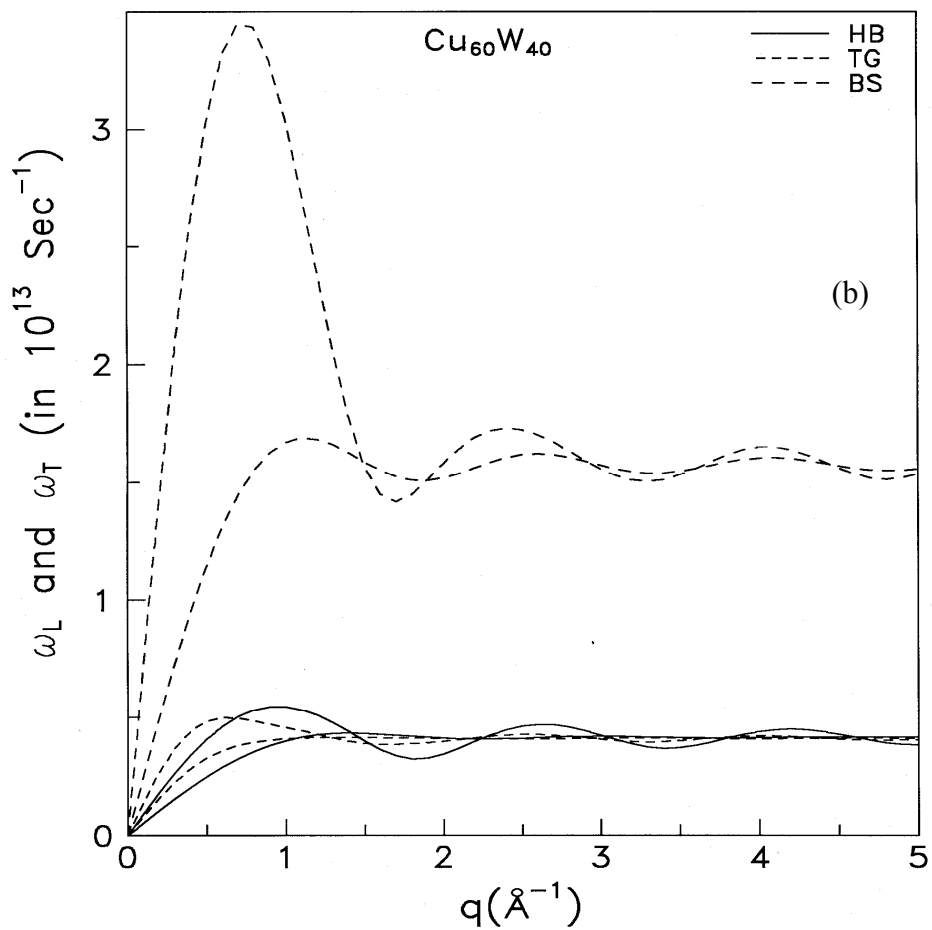
The PDC due to three approaches (HB, TG, BS) of  $\text{Cu}_{57}\text{Zr}_{43}$  glass are shown in Figure 3(a). It is observed that the dispersion of the longitudinal phonons show oscillatory behavior for large  $q$ -values while the transverse phonons show hardly any oscillatory behavior to higher  $q$ -values, i.e. transverse phonon behavior is monotonic at higher  $q$ . The present outcome due to BS approach is higher as compare to other two approaches. The first minimum of the longitudinal branch in HB and TG methods lies at  $q \approx 1.7 \text{ \AA}^{-1}$  while in BS is around  $1.5 \text{ \AA}^{-1}$ . The first crossing position of  $\omega_L$

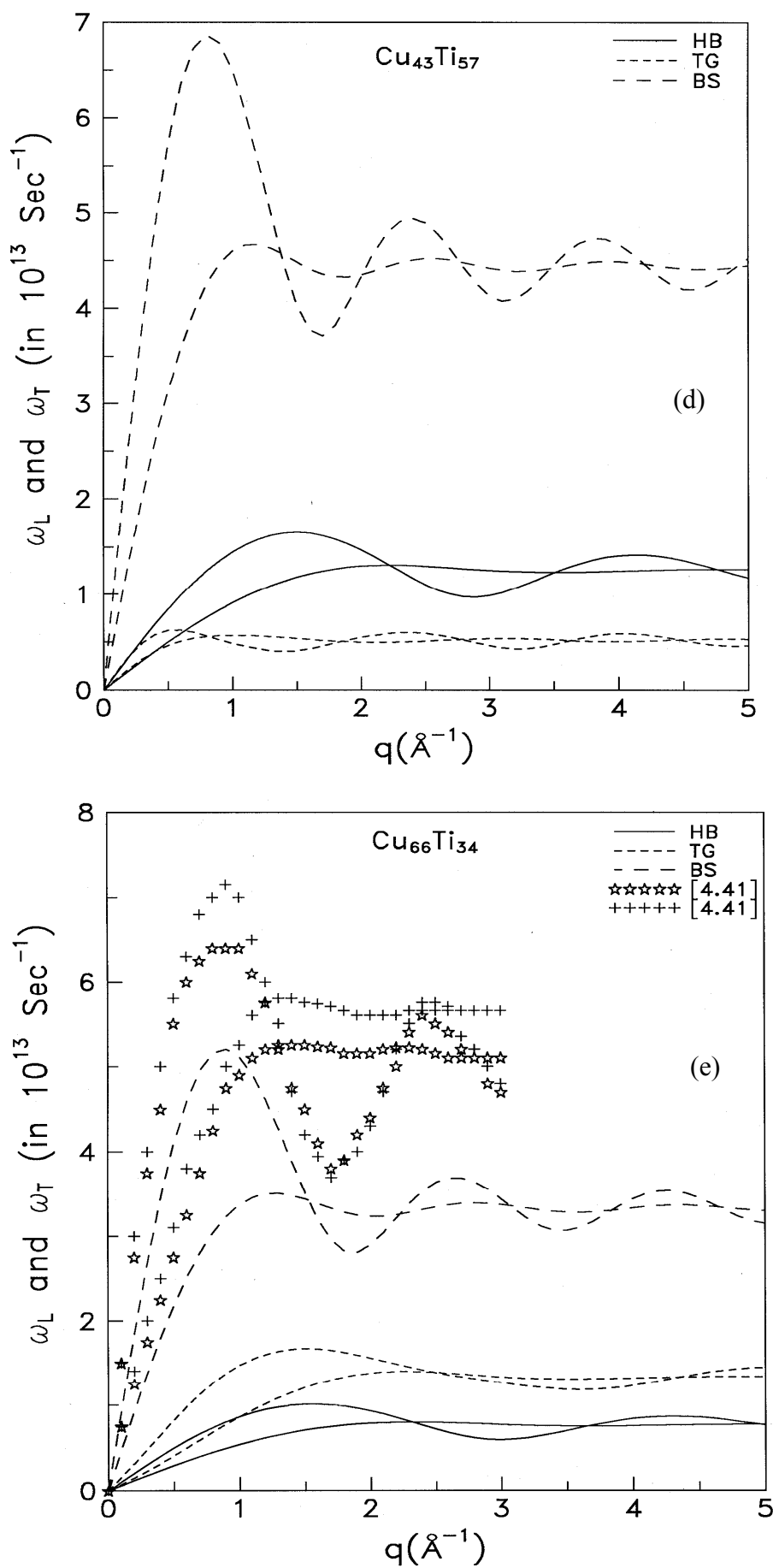
and  $\omega_T$  in the HB, TG and BS approaches is observed respectively at  $1.7\text{\AA}^{-1}$ ,  $1.2\text{\AA}^{-1}$  and  $1.1\text{\AA}^{-1}$ . The PDC of  $\text{Cu}_{57}\text{Zr}_{43}$  glass was also studied by Agarwal et al. [10] using BS approach and various types of screening. The present yielding is compared to those generated by Agarwal et al. [10] and by Kobayashi and Takeuchi [25]. The present outcome due to HB and TG approaches are very low compared to other theoretical results [10, 25]. The structural analysis of  $\text{Cu}_{57}\text{Zr}_{43}$  glass was done by Lamparter et al. [26]. Suck and Rudin [27] have studied the dynamical structure factor, frequency distribution and the dispersion of collective modes of this glass using NIS technique. The PDC due to the three approaches (HB, TG, BS) of  $\text{Cu}_{60}\text{W}_{40}$  glass with S-local field correction function are shown in Figure 3(b). The phonon modes due to BS approach are higher than due to other two approaches. The first minimum in the longitudinal branch falls at  $q \approx 1.8\text{\AA}^{-1}$  for HB,  $q \approx 1.7\text{\AA}^{-1}$  for TG and  $q \approx 1.8\text{\AA}^{-1}$  for BS approach. The first crossing position of both phonon frequencies in the HB, TG and BS approaches is observed, respectively, at  $1.4\text{\AA}^{-1}$ ,  $1.3\text{\AA}^{-1}$  and  $1.4\text{\AA}^{-1}$ . The PDC due to three approaches (HB, TG, BS) of  $\text{Cu}_{33}\text{Y}_{67}$  glass with S-local field correction function are shown in Figure 3(c). The first minimum in the longitudinal branch lies at  $q \approx 2.9\text{\AA}^{-1}$  for HB,  $q \approx 3.4\text{\AA}^{-1}$  for TG and  $q \approx 1.8\text{\AA}^{-1}$  for BS approach. The first crossover location of  $\omega_L$  and  $\omega_T$  in the HB, TG and BS approaches is observed at  $2.1\text{\AA}^{-1}$ ,  $2.4\text{\AA}^{-1}$  and  $1.3\text{\AA}^{-1}$ , respectively. Figure 3(d) is drawn to study the effect of three approaches (HB, TG and BS), where the results of  $\text{Cu}_{43}\text{Ti}_{57}$  glass due to S-local field correction function are shown. Moreover, the present outcome of  $\omega_L$  and  $\omega_T$  due to BS approach are higher than HB and TG approaches. The first immerse in the longitudinal branch falls at  $q \approx 3.1\text{\AA}^{-1}$  for HB,  $q \approx 1.4\text{\AA}^{-1}$  for TG and  $q \approx 1.8\text{\AA}^{-1}$  for BS approach. The first crossing position of  $\omega_L$  and  $\omega_T$  is observed at  $2.2\text{\AA}^{-1}$ ,  $0.8\text{\AA}^{-1}$  and  $1.3\text{\AA}^{-1}$ , respectively, in the HB, TG and BS approaches. The phonon modes due to three approaches proposed by HB, TG and BS with S-screening function of  $\text{Cu}_{66}\text{Ti}_{34}$  glass are displayed in Figure 3(e). Moreover, the height as well as the position of the first peak in both the branches is highly influenced by BS approach in contrast to HB and TG approaches. The first minimum in the longitudinal branch occurs at  $q \approx 3.0\text{\AA}^{-1}$  for HB,  $q \approx 3.6\text{\AA}^{-1}$  for TG and  $q \approx 1.8\text{\AA}^{-1}$  for BS approach. The first crossover position of  $\omega_L$  and  $\omega_T$  in the HB, TG and BS approaches is observed at  $2.2\text{\AA}^{-1}$ ,  $0.8\text{\AA}^{-1}$  and  $1.3\text{\AA}^{-1}$ , respectively. The present results are low in comparison with the reported data of Gupta *et al.* [12].

It is observed from the Figures 3(a)-(e) that the first peak position of longitudinal branch of  $\text{Cu}_{66}\text{Ti}_{34}$  glass is higher while that of  $\text{Cu}_{60}\text{W}_{40}$  glass is lower in comparison with other metallic glasses. The lower dip in the longitudinal branch justifies the correctness and stability of the pair potential. The same results are observed in transverse branch also. Moreover, it is observed from the Figure 4 that the oscillations are more prominent in the longitudinal phonon modes as compared to

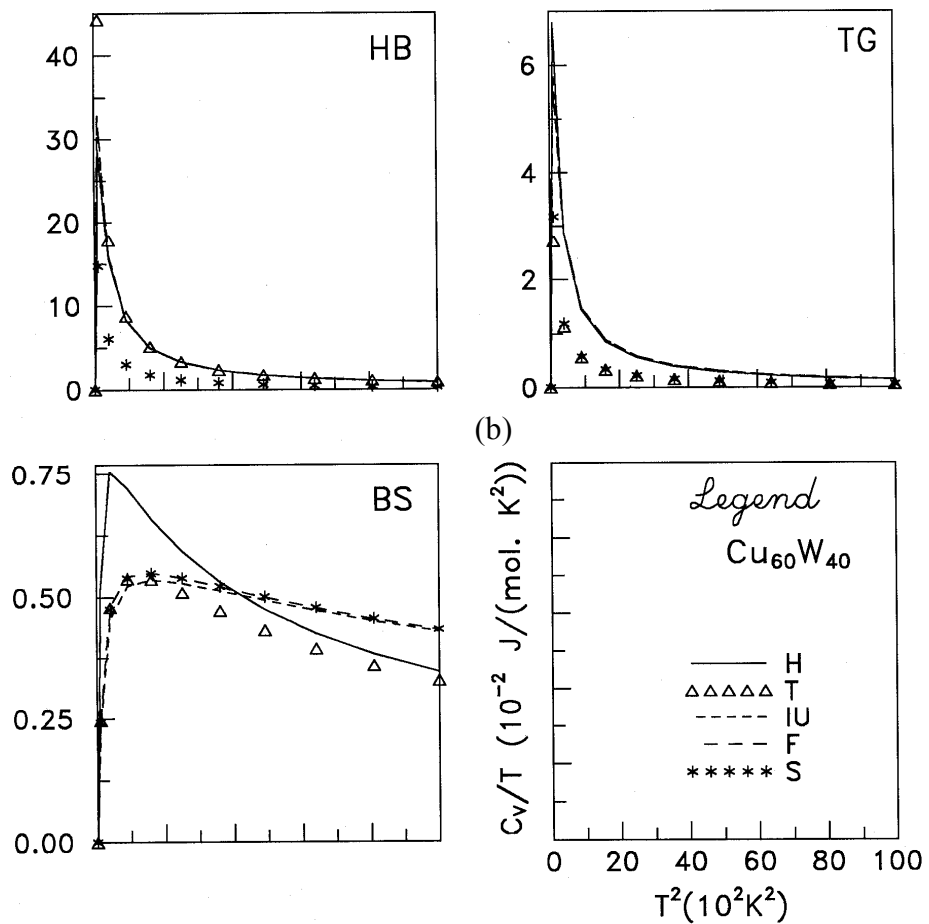
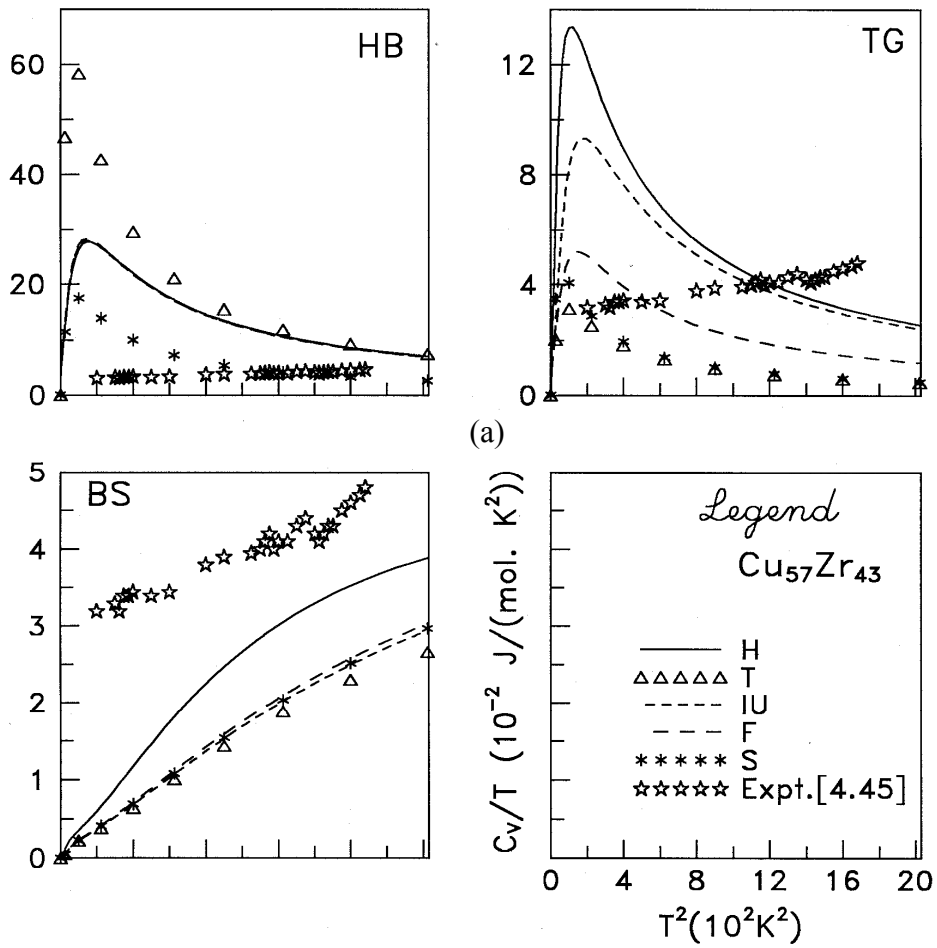
the transverse modes. This shows the existence of collective excitations at larger momentum transfer due to longitudinal phonons only and the instability of the transverse phonons due to the anharmonicity of the atomic vibrations in the metallic systems. Also in the high wave vector region, damping of phonons dominates the transverse mode which is indicating the fluid characteristic of the glass, i.e. transverse phonon behavior is monotonic. Here in transverse branch, the frequencies increase with the wave vector  $q$  and then saturates at  $\approx q=2.0\text{\AA}^{-1}$ , which supports the well-known Thorpe model [27] in which it describes a glass-like solid containing finite liquid cluster. The transverse phonons are absorbed for frequencies larger than the smallest eigen frequencies of the largest cluster.

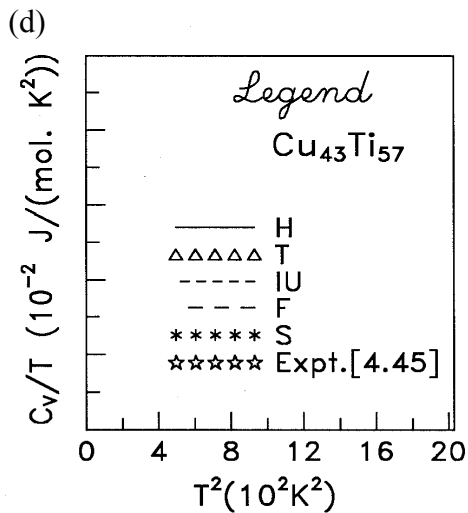
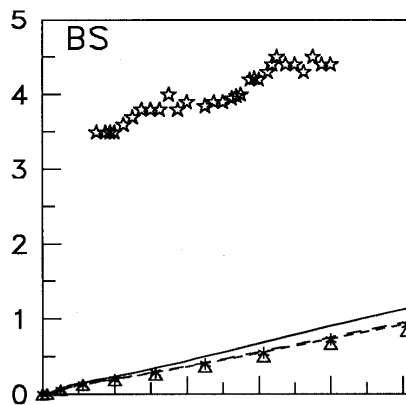
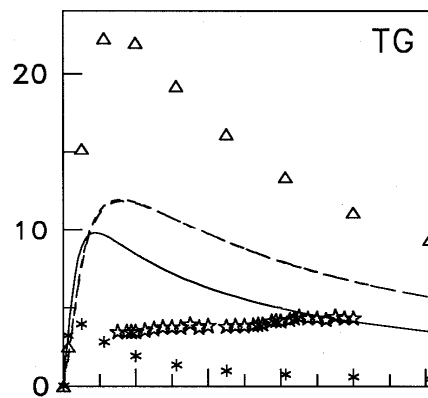
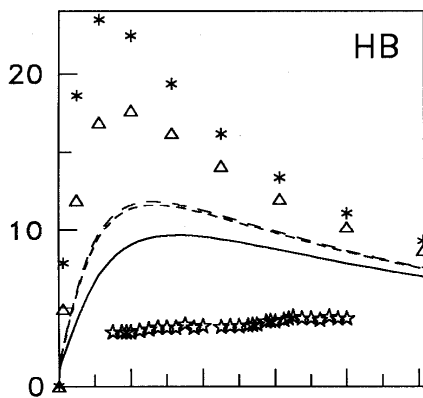
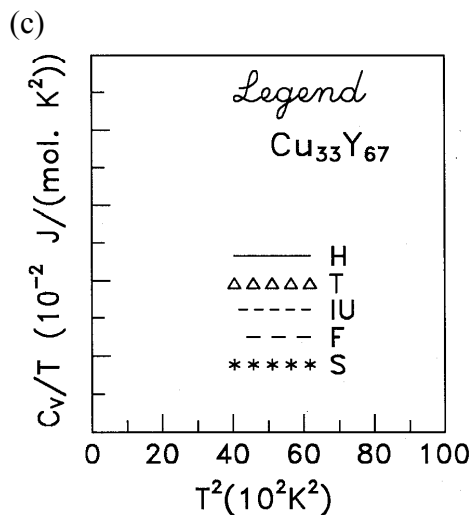
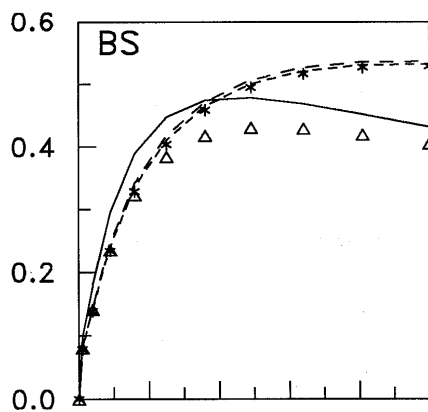
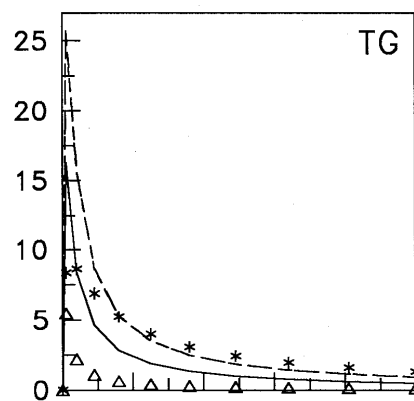
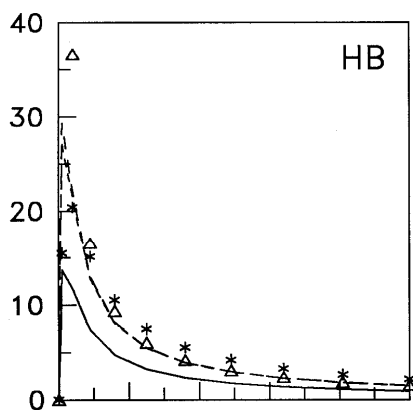






**Fig. 3.** Phonon dispersion curves for (a)  $\text{Cu}_{57}\text{Zr}_{43}$ , (b)  $\text{Cu}_{60}\text{W}_{40}$ , (c)  $\text{Cu}_{33}\text{Y}_{67}$ , (d)  $\text{Cu}_{43}\text{Ti}_{57}$  and (e)  $\text{Cu}_{66}\text{Ti}_{34}$  metallic glasses using HB, TG and BS approaches with S-local field correction function.





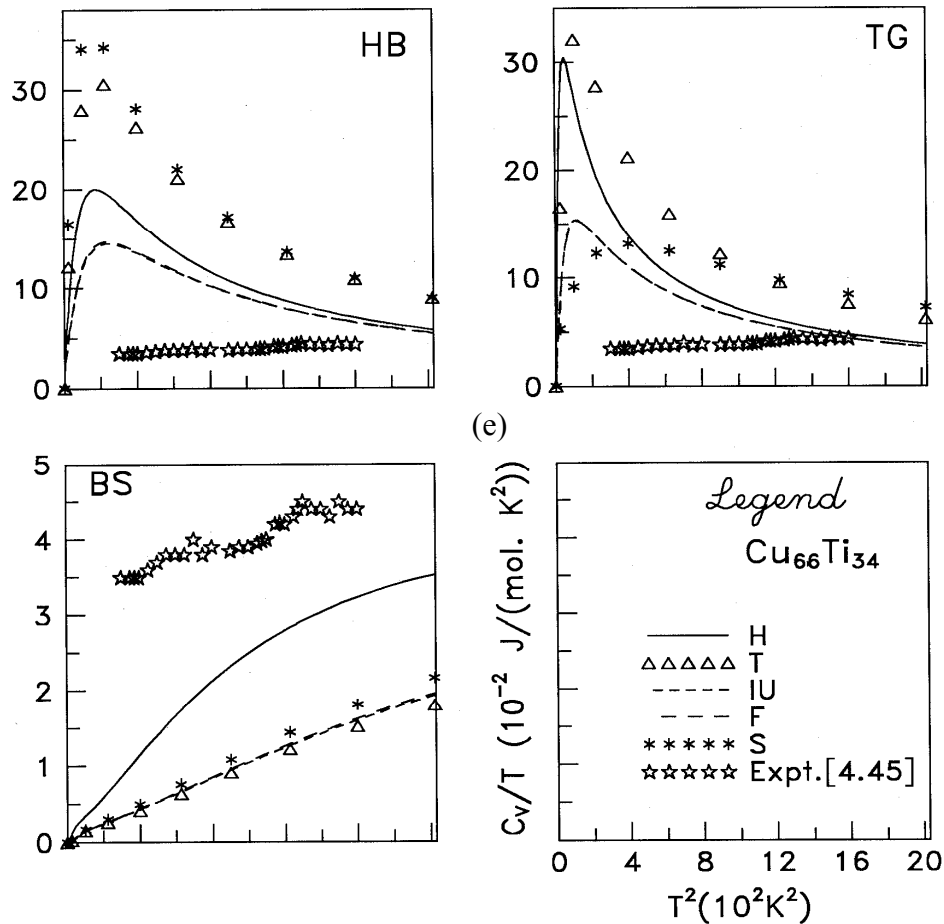


**Fig. 4.** Screening dependence of the low-temperature specific heat for (a)  $\text{Cu}_{57}\text{Zr}_{43}$ , (b)  $\text{Cu}_{60}\text{W}_{40}$ , (c)  $\text{Cu}_{33}\text{Y}_{67}$ , (d)  $\text{Cu}_{43}\text{Ti}_{57}$  and (e)  $\text{Cu}_{66}\text{Ti}_{34}$  metallic glasses computed from HB, TG and BS approaches.

As shown in figures 4(a)-(e) for  $\text{Cu}_{57}\text{Zr}_{43}$ ,  $\text{Cu}_{60}\text{W}_{40}$ ,  $\text{Cu}_{33}\text{Y}_{67}$ ,  $\text{Cu}_{43}\text{Ti}_{57}$  and  $\text{Cu}_{66}\text{Ti}_{34}$  metallic glasses, the exchange and correlation functions also affected in the anomalous behavior (i.e. deviation from the  $T^3$  law), which is observed in the vibrational part of the low-temperature specific heat  $C_V$ . The reason behind the anomalous behavior may be due to the low-frequency modes modify the generalized vibrational density of states of the glass with that of the polycrystal. These modes are mainly responsible for the difference in the temperature dependence of the vibrational part of the specific heat which departs from the normal behavior. The existence of a portion of the spectrum with ‘softer phonons’ (resembling rotons in liquid helium) may be a cause of anomalous behavior of low temperature specific heat  $C_V$ . In the low temperature region, a contribution to the low temperature specific heat  $C_V$  is made by phonons of the initial part of the frequency spectrum. When the temperature reaches a value at which the energy of the thermal motions becomes comparable to the energy of ‘softer phonons’ minimum, an additional contribution appears to heat capacity from the roton portion of the phonon frequency  $\omega(q)$ . The present results of low-temperature specific heat for  $\text{Cu}_{57}\text{Zr}_{43}$ ,  $\text{Cu}_{43}\text{Ti}_{57}$  and  $\text{Cu}_{66}\text{Ti}_{34}$  binary metallic glasses are found to be in qualitative agreement with the available theoretical data [28].

Furthermore, the thermodynamic and elastic properties of Cu-based glassy alloys estimated from the elastic limit of the PDC are tabulated in Tables 2-6. The present results of Cu<sub>57</sub>Zr<sub>43</sub> glass are found lower in line with other theoretical data [10]. The present outcome of these properties of Cu<sub>66</sub>Ti<sub>34</sub> glass due to BS approach is found to be in fair agreement with other such data [12]. As other comparison for these properties of Cu<sub>60</sub>W<sub>40</sub>, Cu<sub>33</sub>Y<sub>67</sub> and Cu<sub>43</sub>Ti<sub>57</sub> glasses is not available, it is difficult to draw any remarks at this stage. But among the three approaches adopted, the outcome due to HB and TG approaches are lower than those due to BS approach. The screening influence on PDC is reflected on these properties also.

**Table 2.** Thermodynamic and Elastic Properties of Cu<sub>57</sub>Zr<sub>43</sub> Glass.

App.	SCR	$v_L \times 10^5$ cm/sec	$v_T \times 10^5$ cm/sec	$B_T \times 10^{11}$ dyne/cm <sup>2</sup>	$G \times 10^{11}$ dyne/cm <sup>2</sup>	$\sigma$	$Y \times 10^{11}$ dyne/cm <sup>2</sup>	$\theta_D$ (K)
<b>HB</b>	<b>H</b>	1.2101	0.6986	0.3825	0.2295	0.2500	0.5738	77.36
	<b>T</b>	0.7974	0.4604	0.1661	0.0997	0.2499	0.2492	50.98
	<b>IU</b>	1.1766	0.6793	0.3616	0.2170	0.2500	0.5424	75.22
	<b>F</b>	1.1702	0.6756	0.3577	0.2146	0.2500	0.5365	74.81
	<b>S</b>	0.3674	0.2121	0.0353	0.0212	0.2500	0.0529	23.49
<b>TG</b>	<b>H</b>	2.0202	1.0505	1.2271	0.5189	0.3147	1.3644	117.25
	<b>T</b>	2.2150	1.3807	1.1118	0.8964	0.1823	2.1195	151.74
	<b>IU</b>	2.3134	1.3398	1.3909	0.8440	0.2476	2.1061	148.31
	<b>F</b>	2.3557	1.3747	1.4246	0.8885	0.2418	2.2068	152.06
	<b>S</b>	1.9624	1.1341	1.0043	0.6047	0.2493	1.5110	125.56
<b>BS</b>	<b>H</b>	5.7243	2.4497	11.6448	2.8216	0.3879	7.8323	276.12
	<b>T</b>	6.2566	2.9663	12.8892	4.1372	0.3550	11.2121	332.85
	<b>IU</b>	6.3072	2.9886	13.1046	4.1997	0.3552	11.3831	335.36
	<b>F</b>	6.2688	2.9476	13.0307	4.0851	0.3581	11.0958	330.89
	<b>S</b>	6.2526	2.9870	12.7886	4.1951	0.3522	11.3447	335.04
<b>Others [10]</b>		–	–	5.81	2.17	–	5.79	339.26
				3.93	2.16		5.49	338.16
				3.98	2.17		5.51	333.39
				5.79	2.16		5.78	333.08
				1.59	2.17		4.48	320.23
				2.22	2.16		4.91	325.17

**Table 3.** Thermodynamic and Elastic Properties of Cu<sub>60</sub>W<sub>40</sub> Glass.

App.	SCR	$\nu_L \times 10^5$ cm/sec	$\nu_T \times 10^5$ cm/sec	$B_T \times 10^{11}$ dyne/cm <sup>2</sup>	$G \times 10^{11}$ dyne/cm <sup>2</sup>	$\sigma$	$Y \times 10^{11}$ dyne/cm <sup>2</sup>	$\theta_D$ (K)
<b>HB</b>	<b>H</b>	0.8702	0.5024	0.3688	0.2213	0.2500	0.5532	60.08
	<b>T</b>	0.6128	0.3538	0.1829	0.1097	0.2500	0.2743	42.31
	<b>IU</b>	0.7740	0.4469	0.2918	0.1751	0.2499	0.4377	53.44
	<b>F</b>	0.7763	0.4482	0.2936	0.1761	0.2499	0.4403	53.60
	<b>S</b>	0.9244	0.5337	0.4162	0.2497	0.2500	0.6244	63.83
<b>TG</b>	<b>H</b>	1.4541	0.7505	1.1953	0.4939	0.3184	1.3022	90.52
	<b>T</b>	1.6114	0.9814	1.1505	0.8444	0.2052	2.0353	116.77
	<b>IU</b>	1.6293	0.9398	1.2948	0.7743	0.2507	1.9369	112.40
	<b>F</b>	1.6620	0.9643	1.3347	0.8153	0.2462	2.0322	115.27
	<b>S</b>	1.4229	0.8213	0.9866	0.5914	0.2502	1.4788	98.22
<b>BS</b>	<b>H</b>	4.4211	1.2382	15.3444	1.3441	0.4574	3.9179	152.12
	<b>T</b>	4.5739	1.5654	15.4767	2.1484	0.4337	6.1601	191.75
	<b>IU</b>	4.6176	1.5978	15.7097	2.2382	0.4320	6.4103	195.68
	<b>F</b>	4.5927	1.5603	15.6467	2.1343	0.4348	6.1244	191.15
	<b>S</b>	4.5603	1.5732	15.3395	2.1697	0.4325	6.2161	192.67

**Table 4.** Thermodynamic and Elastic Properties of Cu<sub>33</sub>Y<sub>67</sub> Glass.

App.	SCR	$\nu_L \times 10^5$ cm/sec	$\nu_T \times 10^5$ cm/sec	$B_T \times 10^{11}$ dyne/cm <sup>2</sup>	$G \times 10^{11}$ dyne/cm <sup>2</sup>	$\sigma$	$Y \times 10^{11}$ dyne/cm <sup>2</sup>	$\theta_D$ (K)
<b>HB</b>	<b>H</b>	1.4391	0.8308	0.5841	0.3504	0.2500	0.8761	92.35
	<b>T</b>	0.2731	0.1576	0.0210	0.0126	0.2503	0.0315	17.52
	<b>IU</b>	1.1827	0.6829	0.3945	0.2367	0.2499	0.5918	75.90
	<b>F</b>	1.1456	0.6614	0.3701	0.2221	0.2500	0.5552	73.51
	<b>S</b>	1.4428	0.8330	0.5871	0.3522	0.2500	0.8806	92.58
<b>TG</b>	<b>H</b>	1.7637	0.7382	1.2103	0.2766	0.3938	0.7711	83.59
	<b>T</b>	1.3964	0.9220	0.4145	0.4316	0.1135	0.9612	101.04
	<b>IU</b>	1.7333	0.9159	0.9572	0.4259	0.3063	1.1127	102.51
	<b>F</b>	1.7411	0.9399	0.9409	0.4485	0.2944	1.1610	105.03
	<b>S</b>	2.1582	0.4686	2.2159	0.1115	0.4753	0.3289	53.61
<b>BS</b>	<b>H</b>	5.8501	3.2656	10.1554	5.4139	0.2737	13.7909	363.99
	<b>T</b>	6.2137	3.5421	11.1080	6.3695	0.2593	16.0422	394.13
	<b>IU</b>	6.2258	3.5345	11.2212	6.3420	0.2622	16.0098	393.41
	<b>F</b>	6.1887	3.5042	11.1315	6.2338	0.2640	15.7595	390.13
	<b>S</b>	6.2365	3.5741	11.0987	6.4849	0.2555	16.2834	397.50

**Table 5.** Thermodynamic and Elastic Properties of Cu<sub>43</sub>Ti<sub>57</sub> Glass.

App.	SCR	$v_L \times 10^5$ cm/sec	$v_T \times 10^5$ cm/sec	$B_T \times 10^{11}$ dyne/cm <sup>2</sup>	$G \times 10^{11}$ dyne/cm <sup>2</sup>	$\sigma$	$Y \times 10^{11}$ dyne/cm <sup>2</sup>	$\theta_D$ (K)
<b>HB</b>	<b>H</b>	2.1693	1.2525	1.2571	0.7543	0.2499	1.8856	155.59
	<b>T</b>	1.5712	0.9072	0.6595	0.3957	0.2499	0.9892	112.70
	<b>IU</b>	1.9557	1.1291	1.0217	0.6130	0.2500	1.5326	140.27
	<b>F</b>	1.9378	1.1188	1.0031	0.6019	0.2499	1.5046	138.99
	<b>S</b>	1.7776	1.0263	0.8441	0.5064	0.2499	1.2661	127.50
<b>TG</b>	<b>H</b>	2.7232	1.1420	2.7296	0.6270	0.3933	1.7473	144.52
	<b>T</b>	2.3885	1.3638	1.5508	0.8943	0.2582	2.2503	169.59
	<b>IU</b>	2.7288	1.3719	2.3737	0.9049	0.3309	2.4087	172.16
	<b>F</b>	2.7506	1.3990	2.3830	0.9410	0.3255	2.4948	175.44
	<b>S</b>	1.9214	1.1629	0.9082	0.6503	0.2110	1.5749	143.83
<b>BS</b>	<b>H</b>	7.8684	3.8467	20.2821	7.1146	0.3430	19.1095	483.49
	<b>T</b>	8.3298	4.2572	21.7431	8.7144	0.3232	23.0623	533.70
	<b>IU</b>	8.3540	4.2588	21.9279	8.7209	0.3244	23.1002	533.98
	<b>F</b>	8.3173	4.2252	21.8170	8.5839	0.3261	22.7660	529.89
	<b>S</b>	8.3463	4.2888	21.7022	8.8443	0.3206	23.3597	537.48

**Table 6.** Thermodynamic and Elastic Properties of Cu<sub>66</sub>Ti<sub>34</sub> Glass.

App.	SCR	$v_L \times 10^5$ cm/sec	$v_T \times 10^5$ cm/sec	$B_T \times 10^{11}$ dyne/cm <sup>2</sup>	$G \times 10^{11}$ dyne/cm <sup>2</sup>	$\sigma$	$Y \times 10^{11}$ dyne/cm <sup>2</sup>	$\theta_D$ (K)
<b>HB</b>	<b>H</b>	1.2921	0.7460	0.5107	0.3064	0.2499	0.7661	94.92
	<b>T</b>	1.1539	0.6662	0.4073	0.2444	0.2500	0.6110	84.77
	<b>IU</b>	1.4988	0.8653	0.6871	0.4123	0.2500	1.0307	110.10
	<b>F</b>	1.4886	0.8594	0.6778	0.4067	0.2500	1.0167	109.35
	<b>S</b>	1.0443	0.6029	0.3336	0.2002	0.2500	0.5004	76.72
<b>TG</b>	<b>H</b>	1.5324	0.5925	1.0352	0.1933	0.4121	0.5459	77.00
	<b>T</b>	1.5611	0.7901	0.8836	0.3437	0.3278	0.9128	101.51
	<b>IU</b>	1.8043	0.8453	1.2680	0.3934	0.3594	1.0697	109.06
	<b>F</b>	1.8128	0.8582	1.2688	0.4056	0.3556	1.0995	110.67
	<b>S</b>	1.5121	0.7259	0.8721	0.2901	0.3503	0.7834	93.53
<b>BS</b>	<b>H</b>	5.4193	2.3135	12.2413	2.9471	0.3886	8.1844	299.68
	<b>T</b>	6.3459	3.2278	14.5243	5.7367	0.3255	15.2079	414.56
	<b>IU</b>	6.4544	3.3031	14.9284	6.0075	0.3226	15.8909	424.07
	<b>F</b>	6.4409	3.2827	14.9310	5.9333	0.3246	15.7179	421.56
	<b>S</b>	6.2335	3.1566	14.0793	5.4865	0.3276	14.5672	405.53
<b>Others [12], [28]</b>		5.24 5.37	2.94 3.07	1.06 1.08	–	–	–	396.98 413.89

The dielectric function plays an important role in the evaluation of potential due to the screening of the electron gas. For this purpose in the present investigation, the local field correction functions due to H, T, IU, F and S are used. Reason for selecting these functions is that H-function does not include exchange and correlation effect and represents only static dielectric function, while T-function cover the overall features of the various local field correction functions proposed before 1972. IU, F and S-functions are recent ones among the existing functions and not exploited rigorously in such study. This helps us to study the relative effects of exchange and correlation in the aforesaid properties. Hence, the five different local field correction functions show variations up to an order of magnitude in all the properties.

In all three approaches, it is very difficult to judge which approaches is best for computations of phonon dynamics of Cu-based metallic glass, because each approximation has its own identity. The HB approach is simplest and older one, which generating consistent results of the phonon data of these glasses, because the HB approaches needs minimum number of parameters. While TG approach is developed upon the quasi-crystalline approximation in which effective force constant depends upon the correlation function for the displacement of atoms and correlation function of displacement itself depends on the phonon frequencies. The BS approach is retained the interatomic interactions effective between the first nearest neighbors only hence, the disorderness of the atoms in the formation of metallic glasses is more which show deviation in magnitude of the PDC and their related properties. From the present study we are concluded that all three approaches are suitable for studying the phonon dynamics of the amorphous materials. Hence, successful application of the model potential with three approaches is observed from the present study.

#### **4. Conclusions**

Lastly it is concluded that in the study of phonon dynamics of metallic glasses, the pair potentials and its derivatives as well as pair correlation function play an important role. In the present computation, the WH form is adopted to generate the pair potentials, which ignores the angular interaction due to partially filled d-bands in transition metals. Most recent model potential with WH model and HB approach produces consistent results of phonon dynamics for all metallic glasses. Hence, the present model potential is suitable for studying the phonon dynamics of five Cu-based metallic glasses, which confirms applicability of the model potential in the aforementioned study. Such study on phonon dynamics of other binary as well as ternary liquid alloys and metallic glasses is in progress, which will be communicated in near future.

## REFERENCES

1. **A.M.Vora, M.H.Patel, P.N.Gajjar, A.R.Jani**, *Solid State Phys.*, **46**, 315 (2003).
2. **P.N.Gajjar, A.M.Vora, A.R.Jani**, *Proc. 9<sup>th</sup> Asia Pacific Physics*, Hanoi, Vietnam, The Gioi Publication, 2006, p. 429.
3. **A.M.Vora**, *Chinese Phys. Lett.*, **23**, 1872 (2006).
4. **A.M.Vora**, *J. Mater. Sci.*, **42**, 935 (2007).
5. **A.M.Vora**, *Acta Phys. Pol. A*, **111**, 859 (2007).
6. **A.M.Vora**, *J. Non-Cryst. Sol.*, **352**, 3217 (2006).
7. **A.M.Vora**, *Front. Mater. Sci.*, **1**, 366 (2007).
8. **A.M.Vora**, *Fizika A*, **16**, 187 (2007).
9. **A.M.Vora**, *Rom. J. Phys.*, **53**, 517 (2008).
10. **P.C.Agarwal, K.A.Aziz, C.M.Kachhava**, *Acta Phys. Hung.*, **71**, 233 (1992); *Phys. Stat. Sol. (b)*, **178**, 303 (1993).
11. **A.B.Bhatia, R.N.Singh**, *Phys. Rev. B*, **31**, 4751 (1985).
12. **N.Gupta, K.C.Jain, N.S.Saxena**, *Phys. Stat. Sol. (b)*, **176**, 81 (1993).
13. **M.A.Engelhardt, S.S.Jaswal, D.J.Sellmyer**, *Phys. Rev. B*, **44**, 12671 (1991).
14. **W.A.Harrison**, *Elementary Electronic Structure*, World Scientific, Singapore, 1999.
15. **R.Taylor**, *J. Phys. F: Met. Phys.*, **8**, 1699 (1978).
16. **S.Ichamaru, K.Utsumi**, *Phys. Rev. B*, **24**, 7385 (1981).
17. **B.Farid, V.Heine, G.Engel, I.J.Robertson**, *Phys. Rev. B*, **48**, 11602 (1993).
18. **A.Sarkar, D.S.Sen, S.Haldar, D.Roy**, *Mod. Phys. Lett. B*, **12**, 639 (1998).
19. **J.Hubbard, J.L.Beeby**, *J. Phys. C: Solid State Phys.*, **2**, 556 (1969).
20. **S.Takeno, M.Goda**, *Prog. Theor. Phys.*, **45**, 331 (1971); *Prog. Theor. Phys.*, **47**, 790 (1972).
21. **A.B.Bhatia, R.N.Singh**, *Phys. Rev. B*, **31**, 4751 (1985).
22. **J.M.Wills, W.A.Harrison**, *Phys. Rev. B*, **28**, 4363 (1983).
23. **N.P.Kovalenko, Y.P.Krasny**, *Physica B*, **162**, 115 (1990).
24. **J.L.Bretonnet, A.Derouiche**, *Phys. Rev. B*, **43**, 8924 (1990).
25. **S.Kobayashi, S.Takeuchi**, *J. Phys. C: Solid State Phys.*, **13**, L969 (1980).
26. **P.Lamparter, S.Steeb, E.Grallath**, *Z. Naturforsch.*, **38a**, 1210 (1983).
27. **J.-B.Suck, H.Rudin**, *Glassy Metals-II: Atomic Structure and Dynamics, Electronic Structure, Magnetic Properties*, **H.-J.Güntherodt, H.Beck (Eds.)**, Springer-Verlag, Berlin, 1983, p. 217.
28. **M.F.Thorpe**, *J. Non-Cryst. Sol.*, **57**, 355 (1983).
29. **D.E.Moody, T.K.Pg**, *Physics of Transition Metals*, Inst. Phys. Conf. Ser. no.55 (chap.13), **P.Rhodes (Ed)**, The Institute Of Physics, Bristol and London, 1981, p. 631.